NAS9-12802
NASA-CR-
LINE ITEM NO. 6
MA-262T
R-9686-1
NASA CR-
144441

# SPACE SHUTTLE

# ORBIT MANEUVERING ENGINE

# REUSABLE THRUST CHAMBER PROGRAM

## FINAL SUMMARY REPORT

13 MARCH 1975



Prepared For

National Aeronautics and Space Administration
Lyndon B. Johnson Space Center
Houston, Texas 77058


Rockwell International
Rocketdyne Division
6633 Canoga Avenue
Canoga Park, California 91304

NASA-CR-

# FINAL SUMMARY REPORT

# SPACE SHUTTLE

# ORBIT MANEUVERING ENGINE

# REUSABLE THRUST CHAMBER PROGRAM

13 MARCH 1975


Prepared By

R. P. Pauckert
SS/OME Principal Engineer

R. D. Tobin

Approved By

R. D. Paster
Program Manager
SS/APS Programs

Rockwell International
Rocketdyne Division
6633 Canoga Avenue
Canoga Park, California 91304

## FOREWORD

This final report summary describes the analytical and experimental studies conducted by the Rocketdyne Division of Rockwell International Corporation from June 1972 through November 1974 under Contract NAS9-12802. The NASA/JSC Program Manager was Merlyn Lausten.

## ABSTRACT

Analyses and preliminary designs of candidate OME propellant combinations and corresponding engine designs were conducted and evaluated in terms of performance, operating limits, program cost, risk, inherent life and maintainability. For the Rocketdyne recommended and NASA approved propellant combination and cooling concept (NTO/MMH regeneratively cooled engine), a demonstration thrust chamber was designed, fabricated, and experimentally evaluated to define operating characteristics and limits. Alternate fuel (50-50) operating characteristics were also investigated with the demonstration chamber.

Adverse operating effects on regenerative cooled operation were evaluated using subscale electrically heated tubes and channels. An investigation of like doublet element characteristics using subscale tests was performed. Full scale 8- and 10-inch diameter like-doublet injectors for the OME were designed, fabricated, and tested. Injector stability was evaluated analytically and experimentally. An integrated (8-inch diameter combustor) thrust chamber simulating the flight configuration was designed, fabricated and tested to further evaluate operating limits of the regenerative cooled design concept. An analytical comparison of 8- and 10-inch OME thrust chamber assemblies was performed using experimental heat flux profiles.

CONTENTS


Introduction . . . . . 1
Program Objectives . . . . . 1
Relationship to Other NASA Efforts . . . . . .1
Method of Approach . . . . . 2
  Program . . . . . 2
  Configuration and Propellant Selection . . . . . 2
  Injector Evaluation . . . . . 6
  Subscale Regenerative Cooling Evaluation . . . . . 11
  Demonstration Thrust Chamber . . . . . 13
  Integrated Thrust Chamber . . . . . 13
  Chamber Diameter Comparison . . . . . 16
Basic Data Generated and Significant Results . . . . . 17
  Program . . . . . 17
  Configuration and Propellant Selection . . . . . 17
  Subscale Regenerative Cooling Evaluation . . . . . 22
  Injector Evaluation . . . . . 26
  Demonstration Thrust Chamber . . . . . 34
  Integrated Thrust Chamber . . . . . 40
  OME Chamber Design Optimization . . . . . 45
  Chamber Diameter Comparison . . . . . 47
Recommendations . . . . . 50
Conclusions . . . . . 51

## ILLUSTRATIONS


1. L/D Injector . . . . . 9
2. Uncooled Thrust Chamber Assembly . . . . . 10
3A. Heated Tube Assembly . . . . . 12
3B. Rectangular Passage 2-D Test Section . . . . . 12
3C. Electrically Heated Panel . . . . . 12
4. Demonstration Thrust Chamber Assembly . . . . . 14
5. Integrated Thrust Chamber . . . . . 15
6. OME Thrust Chamber Assembly . . . . . 21
7. Experimental Burnout Heat Flux Data for MMH . . . . . 23
8. Experimental Burnout Heat Flux Data for MMH . . . . . 23
9. Effect of Completely Plugged Channel on Adjacent Channels Maximum Heat Flux Capability . . . . . 25
10. Summary of Experimental Results for 45 Degree Cant Angle Like-Impinging Doublet Injectors . . . . . 27
11. Effect of Cant Angle and Spacing on c* Efficiency for Like-Doublet Injector With Ambient and Heated Fuel . . . . . 28
12. Like-Doublet Injector Performance - No Film Coolant . . . . . 29
13. Demonstrator OME Thrust Chamber Operating Conditions . . . . . 35
14. OME Engine Performance . . . . . 36
15. Summary of Demonstrator Head Load Data . . . . . 38
16. Integrated Thrust Chamber Engine Installation . . . . . 41
17. Integrated Chamber Performance With Ambient Temperature Propellants . 41
18. Integrated Thrust Chamber Assembly Pressure Drops . . . . . 43
19. Integrated Chamber Heat Load With Ambient Propellants . . . . . 44
20. Effect of Boundary Layer Coolant on Regenerative Chamber Heat Load . . . . . 44
21. Regenerative Coolant Safety Factor Profile . . . . . 46
22. OME Performance With No. 1 L/D Injector . . . . . 46
23. Channel Height Profiles for 8- and 10-Inch Diameter Chambers . . . 48
24. Channel or Land Width Profiles for 8- and 10-Inch Diameter Chambers . . . . . 48

## TABLES


| | | |
|---|---|---|
| 1. | Task Description for SS/OME Reusable Thrust Chamber Program | 3 |
| 1A. | NAS9-12802 Major Hardware Summary | 5 |
| 2. | General Ground Rules | 5 |
| 3. | Like-Doublet Injector Parameters | 7 |
| 4. | Ground Rules | 16 |
| 5. | OME Point Design Characteristics | 18 |
| 6. | Overall OME Design Point Comparison of Cooling Methods | 19 |
| 7. | Summary of Stability Results From Low Contraction Ratio Chamber Tests | 31 |
| 8. | Summary of Stability Results From High Contraction Ratio Chamber Tests | 31 |
| 9. | Thermal Safety Factors Based on Experimental Data | 39 |
| 10. | Summary of Thrust Chamber Assembly Characteristics | 49 |

## INTRODUCTION

The requirements for the space shuttle vehicle dictate an orbital maneuvering propulsion system which is lightweight, exhibits high performance, is insensitive to mission duty cycle, has long life, and is reusable, inspectable, and maintainable. Selection of the optimum propellant combination and engine cooling mode for this system requires the proper compromise between cost, performance, and degree of system sophistication.

An analytical and experimental evaluation of reusable thrust chamber concepts was conducted by Rocketdyne, under Contract NAS9-12802, to determine the optimum configuration for SS/OME application. This report summarizes the contractual effort.

## PROGRAM OBJECTIVES

The primary objective of this program was to evaluate and determine the feasibility of potential reusable thrust chamber concepts for the Space Shuttle Orbit Maneuvering Engine (OME). The program was to provide basic engine data, with emphasis on the thrust chamber, to the potential vehicle contractors to assist in evaluating and selecting various OME configurations.

The program objectives were later expanded to provide basic technical data to support the mainstream OMS and OME programs. This included performance, stability and thermal characteristics data of an OME operating with an alternate injector configuration and with alternate propellants. Transient and off-design operation data were also provided through subscale and full-scale tests.

## RELATIONSHIP TO OTHER NASA EFFORTS

This contractural effort (NAS9-12802) is similar to those conducted under Contracts NAS9-13133 (Aerojet Liquid Rocket Corp.) and NAS9-12803 (Bell Aerospace Co.) in order to evaluate injector and reusable thrust chamber concepts related to the OME and OMS development programs. Related injector stability investigations were concurrently conducted at Rocketdyne under Contract NAS9-12524.

## METHOD OF APPROACH

### PROGRAM

In order to accomplish the stated objectives the program was organized into thirteen tasks. The various task descriptions are summarized in Table / along with the corresponding report numbers summarizing pertinent results.

The approach taken in the program was to first evaluate potential reusable thrust chamber concepts and propellant combinations in order to select an optimum flight design. This was the purpose of Tasks I and II.

Injector performance and stability characteristics were obtained in Tasks VI and XI using both subscale (single-element) and full-scale configurations.

Basic data on the cooling characteristics of candidate amine fuels to aid in configuration selection and later chamber designs were obtained in Tasks VII, IX, and XIII using subscale electrically heated tube assemblies.

In order to prove the feasibility of the selected chamber concept, a demonstrator chamber was designed (Task III), fabricated (Task IV) and tested (Tasks V and VIII).

The demonstrator chamber was followed by a nearly flight type integrated chamber to provide more extensive feasibility evaluation. This chamber was designed and fabricated (Task X) and tested (Task XII) at White Sands Test Facility.

A comparison of 8- and 10-inch diameter chambers was made in Task X in order to determine the optimum configuration for OME application.

The method of approach utilized in each of the six primary areas of investigation discussed above follows. The major hardware fabricated is summarized in Table 1a.

### CONFIGURATION AND PROPELLANT SELECTION

Detailed point designs were generated for both film and regeneratively cooled thrust chambers which appeared promising for application to the SSME. The basic ground rules are given in Table 2. The propellant combinations considered were NTO/MMH, NTO/50-50, LOX/MMH, LOX/50-50, LOX/RP-1, and LOX/$C_3H_8$. Designs were generated for each propellant

## TABLE 1. TASK DESCRIPTION FOR SS/OME REUSABLE THRUST CHAMBER PROGRAM

| Task No. | Title | Task Description | Report Number |
|---|---|---|---|
| I | Reusable Thrust Chamber Evaluation | Design and analysis of promising reusable thrust chamber concepts applicable to the SS/OME with NTO/MMH and NTO/50-50 propellants. | 128675<br>141671 |
| II | Alternate OME Propellant Combinations | Design and analysis of promising reusable thrust chamber concepts applicable to the SS/OME with LOX/amine and LOX/hydrocarbon propellants. | Same |
| III | Demonstration Thrust Chamber Design | Detailed design of an experimental thrust chamber to demonstrate critical design, fabrication, and operating areas of regeneratively cooled reusable chamber. | 141673 |
| IV | Demonstration Thrust Chamber Fabrication | Fabrication of demonstration chamber. | None |
| V | Demonstration Thrust Chamber Testing | Hot-fire testing of demonstration chamber at simulated altitude over a range of operating conditions with NTO/MMH propellants. | 140321 |
| VI | Hot Fire Element Investigation | Subscale injector hot-fire tests, performance, thermal and stability evaluation of like-doublet and triplet element configurations for REGEN chamber. | 141677 |
| VII | Heat Transfer Testing | Characterize the cooling capability of MMH and 50-50 fuels at OME type operating conditions using electrically heated test sections. | 141672 |
| VIII | Alternate Propellant Demonstration | Hot-fire testing of demonstration chamber at simulated altitude over a range of operating conditions with NTO/50-50. Compare with Task V results. | 140321 |
| IX | Adverse Operating Conditions | Investigate effects of hot manifold starts and helium ingestion using electrically heated single tube test sections. | 134282 |
| X | Integrated Thrust Chamber Fabrication | Design and fabricate an 8-inch diameter integrated thrust chamber assembly which simulates the performance, thermal, and hydraulic characteristics of OME flight configuration. Analytically compare 8- and 10-inch diameter thrust chamber assembly. | 141675 |
| XI | OME Injector | Experimentally determine stability of existing 8-inch diameter injector. Design, fabricate and test 10-inch diameter injector. Conduct stability analysis including review of existing data. | 140358<br>141674<br>141676 |
| XII | Integrated Thrust Chamber Test | Experimentally evaluate operating characteristics of OME ITC. Evaluate steady-state, start, shutdown and restart characteristics. | 132256<br>140250 |
| XIII | Subscale Helium Ingestion and Two Dimensional Heating Tests | Evaluate transient and steady-state helium ingestion capabilities of OME thrust chamber using electrically heated single and multiple channels. Evaluate 2-D conduction and plugged channel operating characteristics with same test sections. | 141560 |

TABLE 1A

NAS9-12802 MAJOR HARDWARE SUMMARY

| COMPONENT | DESIGN CHARACTERISTICS | MEASURED CHARACTERISTICS | TEST EXPOSURE No. of Starts | TEST EXPOSURE Total Duration |
|---|---|---|---|---|
| Demonstrator Thrust Chamber | Flight type jacket, 180 channels, 0.060 inch constant channel width(stepped to 0.120 inch in nozzle), 0.040 inch minimum land width, 0.078-0.175 inch channel height profile, thermal safety factor > 2 at nominal conditions, predicted life - 4000 cycles. Spun/machined 321 CRES liner with 0.030 inch electroformed nickel closeout. Combuster: 8 inch I.D. X 14.7 inch with $\epsilon_c$=2. Silicide-coated columbium nozzle for 7<E≤9. Separate fuel FLC injector manifold. | 13 psi jacket pressure drop and 700 BTU/sec heat load at nominal conditions with L/D #1 injector. | 112 | 1042 |
| Integrated Thrust Chamber | Flight type (except inlet manifold) .120 constant width (0.114 inch) channels. Channel height profile (0.042-0.146 inches). 0.038 inch minimum land width. Thermal safety factor nominally > 2. Predicted life 5000 cycles, 304L CRES liner with 0.025 inch electroformed nickel closeout. Acoustic cavities part of chamber. | 15 psi jacket pressure drop and 750 BTU/sec chamber heat load at nominal conditions with L/D #1 injector. | 156 | 1190 |
| L/D #1 Injector | 8.2 inch diameter. 186 like doublet elements. Minimum orifice diameters; oxidizer - 0.028 inches, fuel - 0.032 inches. 68 boundary layer coolant orifices (0.020 inch diameter). Flight type .321 CRES material. Electrodischarge machined orifices (EDM). | Pressure drops at nominal conditions; Oxidizer - 56 psi, fuel - 61 psi. Nominal vacuum $I_s$ - 310 sec. | 302 | 1775 |
| L/D #4 Injector | 10 inch diameter. 229 like doublet elements minimum orifice diameters: Oxidizer - 0.029 inches; fuel - 0.031 inches. Flight type 321 CRES. EDM orifices. | Approximate pressure drops at nominal conditions • Oxidizer - 65 psi; fuel - 50 psi | 28 | 108 |

TABLE 2

GENERAL GROUND RULES

| | |
|---|---|
| ● ENGINE ASSEMBLY INCLUDES | THRUST CHAMBER |
| | INJECTOR (IGNITER FOR LOX) |
| | THROAT GIMBAL RING (7 DEGREE) |
| | SERIES/PARALLEL VALVE |
| | DUCTS |
| ● COOLING CONCEPTS | REGENERATIVE AND DUMP/FILM |
| ● MINIMUM CYCLE LIFE CAPABILITY | 1000 CYCLES |
| ● OPERATING DURATION | 15 HOURS |
| ● CONTRACTION AREA RATIO | 2 |
| ● NOZZLE LENGTH | 70 PERCENT |
| ● RADIATION SKIRT MATERIAL | COATED COLUMBIUM $1600 < T \leq 2400$ F |
| | COATED TITANIUM $T \leq 1600$ F |
| ● VALVE AND INJECTOR MATERIAL | CRES |
| ● VALVE ACTUATION | PNEUMATIC |

combination. Parametric data were generated, based on perturbing these point designs, describing engine weights, performance, inlet pressures, envelope, reliability, maintainability, and costs. The total engine was considered in these evaluations and included the thrust chamber assembly, propellant valve and ducts, gimbaling actuator ring, and bearing, and the electrical and pneumatic systems.

The results of these studies were published (NASA-CR- ) to aid NASA and potential orbiter and OMS contractors in configuration selection and evaluation.

## INJECTOR EVALUATION

Subscale and full-scale injectors were designed, fabricated, and tested extensively in order to characterize like doublet and triplet element configurations in terms of performance and heat transfer. Stability model tests were also conducted and analysis and evaluation of all available OME experimental data were made.

### Subscale Injector Element Characterization

Hot-fire tests were conducted with single element configuration in a heat sink chamber. The tests were conducted: (1) determine the optimum like-doublet element geometry for operation at conditions consistent with a fuel regeneratively cooled OME, and (2) to further investigate the sensitivity of the triplet element injector to hot fuels. For the like-doublet element injector, tests were conducted to determine: (1) the optimum cant angle and spacing, (2) the minimum number of elements required, (3) the possible turbulent mixing effect as a function of chamber length, (4) the influence of fuel and oxidizer temperatures on performance, and (5) the effects of chamber pressure and mixture ratio on C* efficiency.

### Full-Scale Injector Element Characterization

Like-doublet elements were designed and fabricated for OME thrust chambers having contraction area ratios of 2 and 3. The corresponding injector diameters were 8.2 inches and 10 inches. The injector design parameters are shown in Table . Primary differences between the injectors, in addition to their diameters, is the number of elements and the element spacing and cant angle. In both cases, the number of elements represented a maximum number which could be conveniently fabricated for the particular element geometry and injector diameter. The spacing and cant angle for the L/D #1

TABLE 3

LIKE-DOUBLET INJECTOR PARAMETERS

| | L/D #4 | L/D #1 |
|---|---|---|
| Face Diameter, Inches | 10.0 | 8.2 |
| Number of Elements | 229 | 186 |
| Orifice Forming | EDM | EDM |
| Diameter of BLC Orifices (68), Inches | - | 0.02[illegible] |
| Diameter of Fuel Element, Inches | 0.0294 | 0.028-0.033 |
| Diameter of Oxidizer Element, Inches | 0.0309 | 0.032-0.038 |
| O-F Element Spacing, Inches | 0.45 | 0.19 |
| Impingement Height, Inches | 0.101 | 0.188 |
| Cant Angle, Degrees | 45 | 22.5 |
| Nominal Fuel $\Delta P$, PSI | 45 | 62 |
| Nominal Oxidizer $\Delta P$, PSI | 55 | 55 |
| Radial Sequence | O-F-O-F | O-O-F-F |
| Stabilization | Acoustic Cavities and Fuel Manifold Dams | Acoustic Cavities and Fuel Manifold Dams |
| Injector Material | 321 CRES | 321 CRES |

injector were determined from previous injector experience. The values of these parameters for the L/D #4 injector were determined by the subscale tests.

Another important difference between these injectors is the radial sequencing of the fans. In both cases oxidizer fans impinge on fuel fans. However, for the L/D #1 injector each propellant fan is adjacent to a fan of the same propellant on its nonimpinging side. This maximizes interelement mixing for sprays which pass radially through the primary mixing zone without ineraction with the opposite propellant in that zone. On the other hand, the radial sequence used with injector L/D #4 in which the fuel and oxidizer fans are radially alternated, provides maximum interelement mixing in the event of propellant blowapart in the primary mixing region.

Figure 1 shows photographs of the two injectors. Both 8- and 10-inch injectors were first tested in solid workhorse thrust chambers under sea level conditions to determine performance, thermal, and stability characteristics. A typical hardware cross section is shown in Fig. 2 . A combustion chamber consisted of a converging-diverging section and a cylindrical section, one or more of which were used to vary the distance from the injector to the throat. The combustion chamber sections were instrumented with thermally isolated outside wall temperature measurements. The heat flux profile was deduced from the transient temperatures recorded by these thermocouples. Bombs were detonated and high response chamber pressure measurements were made approximately three inches from the injector face to provide stability data for each injector. The initial tests on the L/D #1 injector were made with boundary layer coolant supplied by a separate manifold between the injector and combustion chamber. Subsequent tests on the L/D #1 injector were made with BLC supplied through orifices drilled around the periphery of the injector. No BLC was used with the L/D #4 injector.

In addition to the tests conducted with the solid wall thrust chambers, numerous tests were conducted with the L/D #1 injector in the demonstrator and integrated regeneratively cooled thrust chambers. Results of these tests are reported in the two sections entitled, "Demonstrator Thrust Chamber" and "Integrated Thrust Chamber". A total duration of approximately 1775 seconds was accumulated on the injector during 302 tests.

Stability Analysis and Tests. Under Task XI of the program stability tests and analysis were conducted to define stability characteristics of various OME chamber/injector configurations and to determine the effectiveness of various acoustic cavity designs. The effort comprised two series of full-scale stability rating tests, bench-scale acoustic modeling tests, and analyses of data from tests conducted by Rocketdyne and other OME technology contractors.

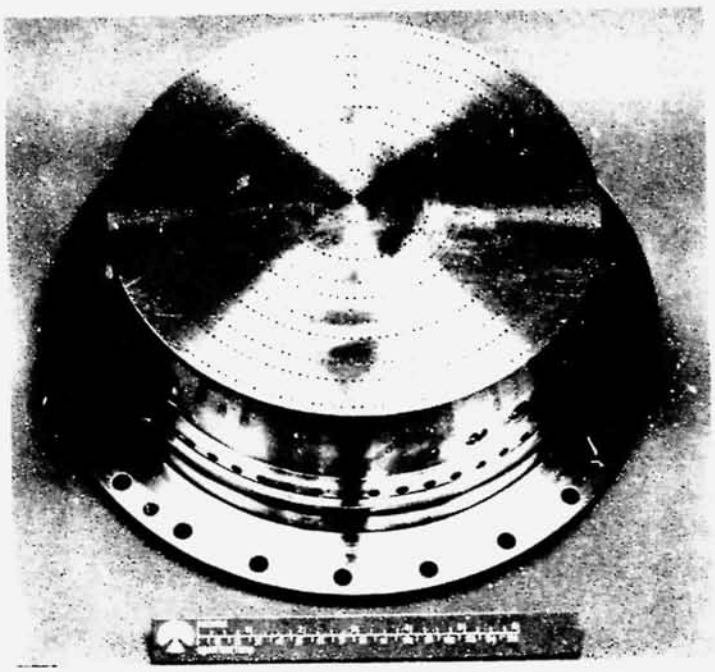

NO. 1

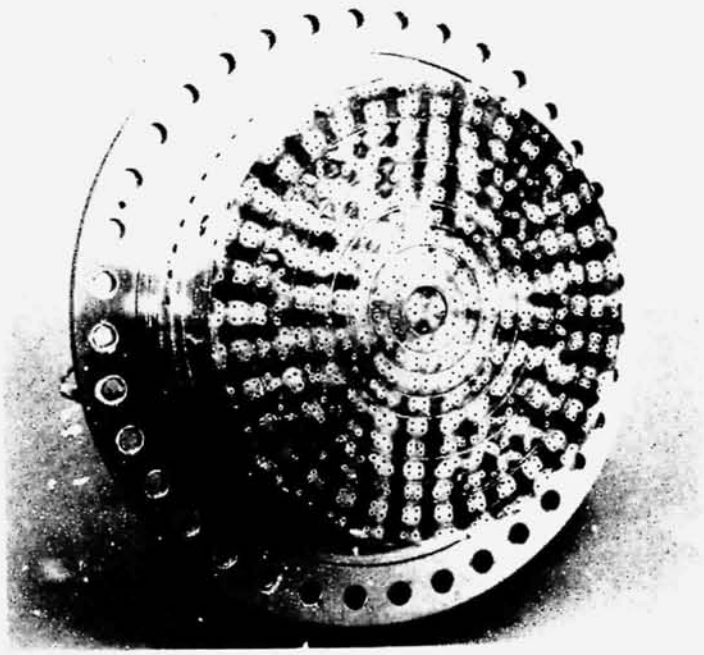

No. 4

Figure 1. L/D Injector

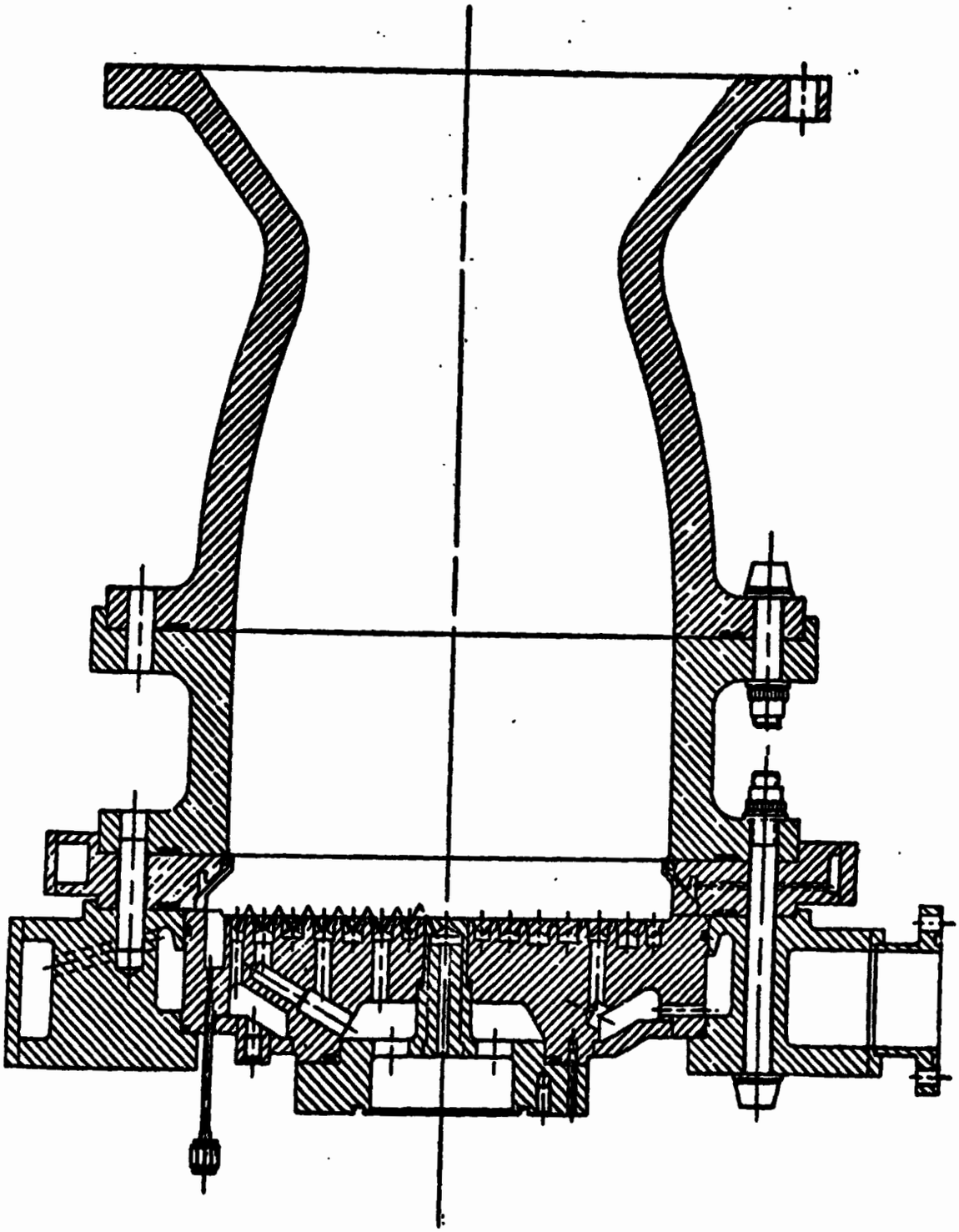

Figure 2. Uncooled Thrust Chamber Assembly

Full-Scale Tests. The previously described L/D #1 and L/D #4 injectors were used for the full-scale test program. The L/D #1 injector had been used previously for extensive nonstability related testing, although a few stability rating tests had been made before the BLC injection orifices were drilled in the injector. These tests were stable with the acoustic cavity being used. Related stability rating tests had been made on Contract NAS9-12525 with a somewhat similar injector, L/D #2, which showed that an acoustic cavity was required to achieve stability.

Solid wall combustion chambers typical of that shown in Fig. 2 were used. For the tests conducted under this contract, the BLC injector ring was eliminated. The L/D #1 injector had 68 equispaced 0.020-inch diameter orifices near its circumference; no BLC was used for the tests with the L/D #4 injector.

The acoustic cavities were formed between the injector and removable rings, to facilitate modification of the cavity configurations. The acoustic cavities used for all of these tests had a contoured entrance. In addition to the normal thrust, pressure, flow, and temperature instrumentation special temperature and high-frequency pressure instrumentation was used. The chambers were instrumented with three high frequency response pressure transducers. Gas temperatures were measured in the acoustic cavities with exposed-junction thermocouples.

Acoustic Model Testing. Two kinds of acoustic model tests were made, one with relatively detailed models of the acoustic cavities only and the second with a model of the combustion chamber containing acoustic cavities. The tests with the detailed cavity models were made to measure the effective acoustic depth of these cavities associated with the entrance region. The tests with the chamber model were made to measure the influence of the cavities on the acoustic modes of the chamber. Each kind of model was excited with an acoustic driver and the model response was measured with a microphone. The frequencies corresponding to maximum microphone response were interpreted as the resonant frequencies of the models.

## SUBSCALE REGENERATIVE COOLING EVALUATION

The cooling capability of MMH and 50-50 fuels was determined using electrically heated circular steel tubes and rectangular channels as shown in Fig. 3. The circular tube provides a uniform circumferential heat flux to the coolant and, as such, provides basic cooling data relatively independent of geometry. The rectangular channel test section incorporated a copper heating strip along one surface so as to more closely simulate the asymmetric heating that occurs in a thrust chamber. The 2-D heat transfer results were modeled on the computer using the basic round tube correlation.

The electrically heated test sections were also utilized to investigate adverse operating conditions such as hot-starts and helium ingestion. In the former case the test sections were preheated to selected temperature levels and the fuel was then introduced at velocities and flowrates

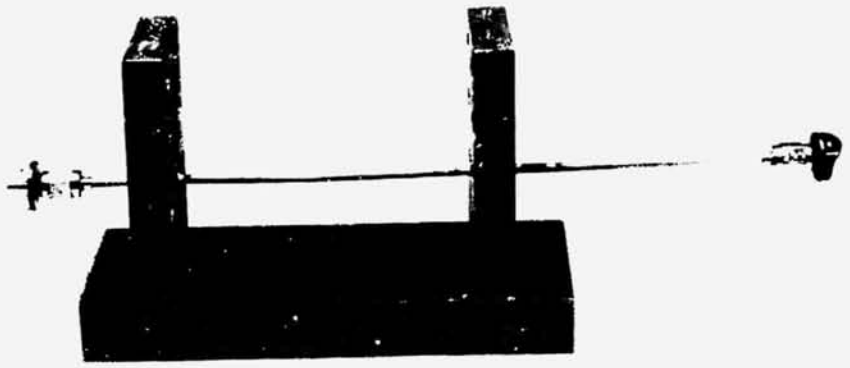

Figure 3A. Heated Tube Assembly

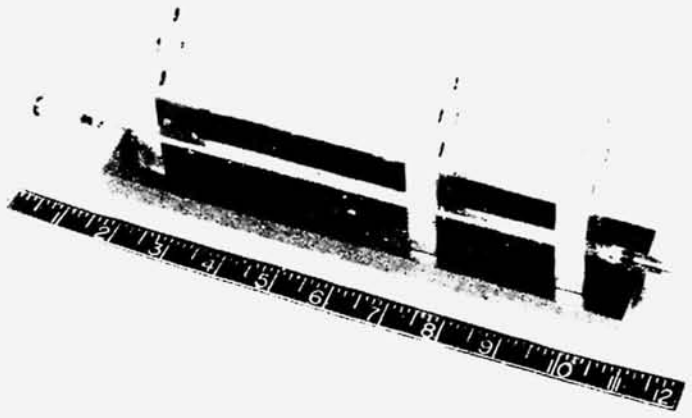

Figure 3B. Rectangular Passage 2-D Test Section

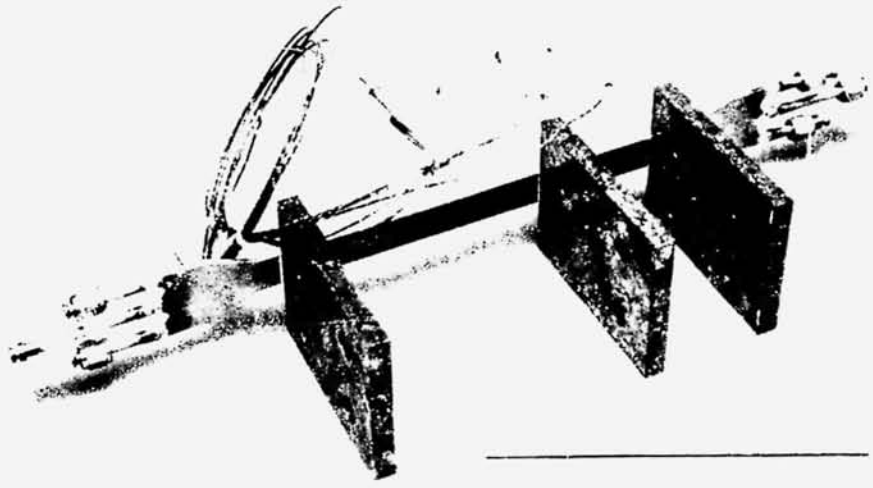

Figure 3C. Electrically Heated Panel

simulating start conditions. Helium ingestion was accomplished in both discrete bubble and froth-type flows at various heat flux levels. These flows were visually observed through a sight tube immediately downstream of the test section.

A three-channel panel (Fig. 3c) similar to the single channel design was used to investigate effects of adjacent channel cooling on helium ingestion and plugged channel operation. In these tests the center of the three channels utilized a separate flow circuit such that flowrate could be reduced or helium ingested in this channel.

DEMONSTRATION THRUST CHAMBER

In order to investigate the feasibility of the regeneratively cooled chamber concept, a demonstration chamber was designed, fabricated and tested. The basic chamber is shown in Fig. 4. This chamber had 180 coolant passages which were 0.060 inches wide with heights ranging from 0.078 to 0.175 inches. The nominal pressure drop for this chamber was 13 psi. The chamber cooling passages simulate flight-type design in terms of geometry and pressure drop. The head-end, however, incorporates a separate outlet manifold and film coolant ring so that regenerative coolant and film coolant flowrates can be varied to obtain basic chamber cooling data. A short columbium radiation cooled nozzle is included to determine nozzle operating temperatures and to simulate soakback conditions.

The chamber was instrumented to obtain coolant bulk temperature rise, back wall temperature profiles, coolant pressure drop, and performance and stability characteristics.

The chamber was tested over a range of chamber pressure and mixture ratios at Rocketdyne (CTL IV) and White Sands Test Facility. The dump and regenerative cooling modes were used at Rocketdyne. Regenerative cooling was used at WSTF. Film coolant flowrates were varied independently by means of suitable orificing. Start transient and soakout conditions as well as off-design operation were also investigated.

INTEGRATED THRUST CHAMBER

In order to more carefully evaluate transient operating characteristics, a chamber was designed and fabricated with a nearly flight-type head-end configuration as shown in Fig. 5. The design incorporates the acoustic cavities and dams integral with the regeneratively cooled chamber. The film coolant is supplied from the primary injector.

The ITC was tested in two phases at WSTF. The first phase was primarily oriented to obtain steady state performance data in vacuum with a full 72:1 area ratio steel heat sink nozzle. The second test phase was conducted to obtain OME start, shutdown, and restart data. Operation under throttled conditions and without boundary layer cooling was also demonstrated during the second test series. Instrumentation was essentially similar to that used in demonstration chamber tests.

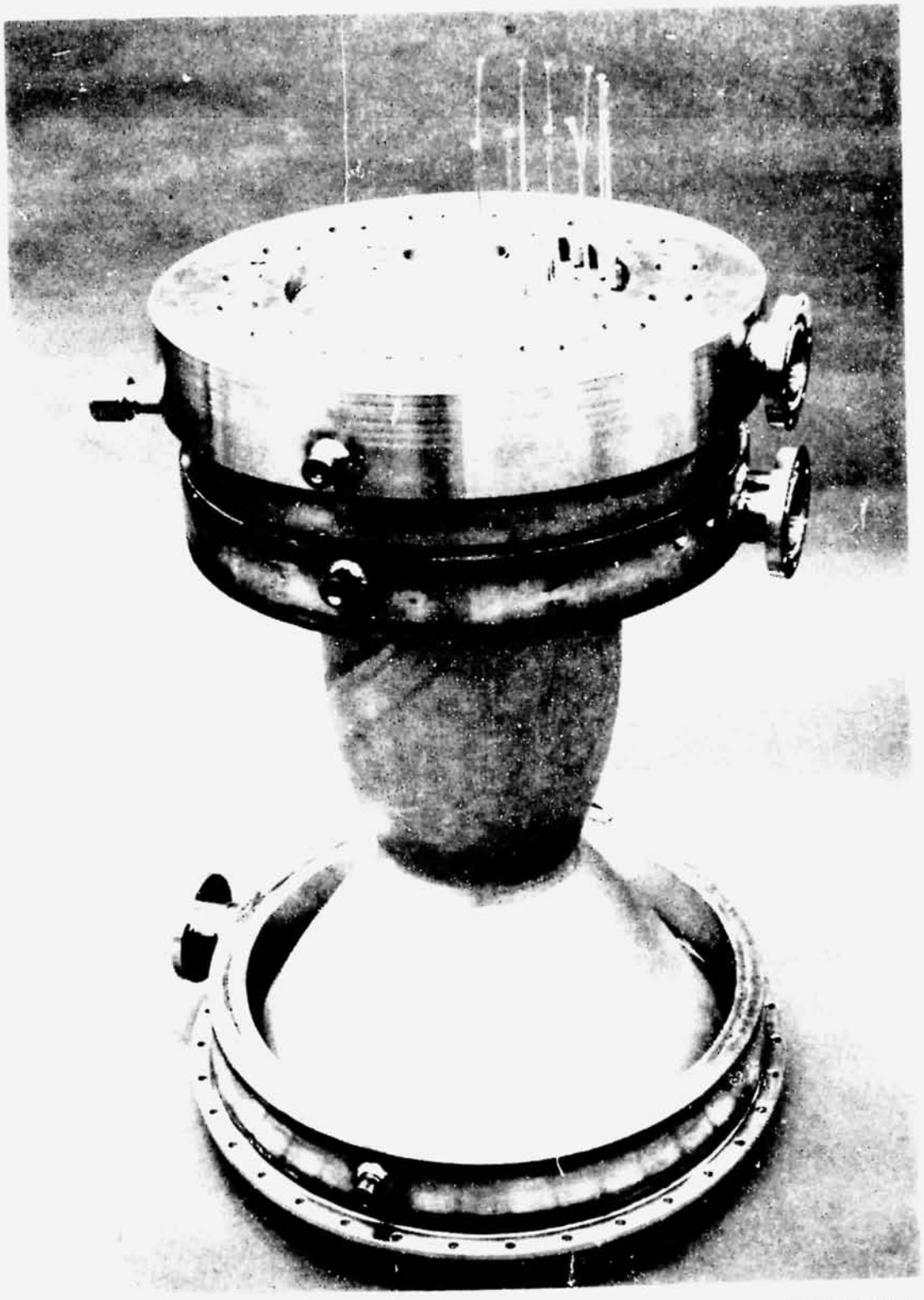

1S032-3/29/73-C1D

Figure 4. Demonstration Thrust Chamber Assembly

| | |
|---|---|
| INJECTOR END DIAMETER, INCHES | 8 |
| INJECTOR-TO-THROAT LENGTH, INCHES | 14.7 |
| CHARACTERISTIC LENGTH, INCHES | 26.5 |
| AREA RATIO (W/O NOZZLE EXTENSION) | 7 |
| LINER MATERIAL | 304L CRES |
| OUTER WALL MATERIAL | ELF. NICKEL |
| NUMBER OF CHANNELS | 120 |
| TYPE OF CHANNEL | CONST. WIDTH STEPPED |

Figure 5, Integrated Thrust Chamber

## CHAMBER DIAMETER COMPARISON

An objective of Task X was to compare 8- and 10-inch diameter chamber configurations (contraction ratio = 2 and 3, respectively) in terms of system weight, pressure drop and performance. Also the advantages of using a constant land width fabrication technique in comparison to the nominal constant channel width design was to be evaluated.

The initial Rocketdyne regeneratively cooled OME design was perturbed to determine the effects of changing the design contraction ratio and fabrication technique. Three chamber configurations were investigated: (1) contraction ratio of 2 and constant channel width; (2) contraction ratio of 2 and constant land width; and (3) contraction ratio of 3 and constant width.

The basic ground rules for the study are summarized in Table 4. Experimental heat flux profiles were utilized based on data from Rocketdyne ($\varepsilon_c$ = 2) and Bell Aerosystems ($\varepsilon_c$ = 3). Only the regeneratively cooled chamber, radiation cooled nozzle and injector were considered in the weight analysis.

Guided by previous design effort 120 channels were selected for all chambers. A minimum land width at the throat of 0.040 inch was selected based on fabrication ease. Hot-wall and closeout thicknesses of 0.030 inch were utilized on all chambers for consistency. Coolant safety factors were evaluated based on 2-D thermal analysis where applicable (e.g., wide injector-end lands in constant channel width design).

TABLE 4. GROUND RULES

Components: Injector, Chamber, Nozzle

Regeneratively Cooled Nozzle ARea Ratio: 7

Nozzle Area Ratio: 72

- Chamber Length for $\varepsilon_c$ = 2: 14.7 inches
- Nozzle Percent Length for $\varepsilon_c$ = 2: 70
- Chamber Length for $\varepsilon_c$ = 3: 12 inches
- Nozzle Percent Length for $\varepsilon_c$ = 3: 73

Injector P Not Dependent on $\varepsilon_c$

Experimental Heat Flux Profiles

Hot and Cold Wall Thicknesses: 0.030 inch

REGEN Safety Factor: 1.5 at Off Design

Off-Design Conditions: $P_c$ = 120 psia
MR = 1.73
$T_{In}$ = 100 F

## BASIC DATA GENERATED AND SIGNIFICANT RESULTS

### PROGRAM

In terms of the overall program the most significant result is the proven feasibility of the regenerative cooled reusable thrust chamber concept for OME application. Successful operation was obtained over a wide range of steady-state (no bombs were detonated in the chamber) operating conditions with no evidence of injector instability or chamber overheating. The chamber can be safely operated over any start, shutdown, restart sequence currently envisioned for the OME. A summary of the significant results obtained in each major portion of the program are discussed in the following pages.

### CONFIGURATION AND PROPELLANT SELECTION

#### Design Comparison Summary

A summary of OME point design characteristics for the various propellants and cooling methods are listed in Table 5 for engines with a 50 inch static external exit diameter. Mixture ratios for engines using NTO/MMH and NTO/50-50 are based on equal propellant tank volumes. For the other propellants the mixture ratio is that which yields maximum delivered specific impulse. Engine lengths are measured from the top of the oxidizer duct to the end of the radiation cooled nozzle; combustor lengths from the injector face to the throat plane. Engine inlet pressures are the pressures at the vehicle connect point and include the pressure drops through all engine components.

The regeneratively cooled engines deliver higher specific impulse performance than the film cooled engines and have higher engine weights and fuel inlet pressures.

The effects of specific impulse, engine weights, and inlet pressure on loaded OMS weight were determined using nominal OMS weight and trade factors. The results of the cooling method comparison shown in Table  indicate that the regeneratively cooled engine results in lower OMS weights than the film cooled engine. The results of the propellant comparison for regeneratively cooled OME systems are also shown in Table 6. NTO/50-50 yields a slightly lower system weight than NTO/MMH. The lowest system weight is achieved with LOX/MMH.

Life capabilities were determined for the regeneratively cooled and dump/film cooled thrust chambers. Each concept is limited by a different damage mechanism: the regeneratively cooled chambers by fatigue; the dump/film cooled chambers by creep. Life capability did not critically influence design selection since all designs exceeded the required 1000-cycle life requirement (with a Safety Factor = 4.0).

## TABLE 5. OME POINT DESIGN CHARACTERISTICS

| Propellant | NTO/50-50 | NTO/50-50 | NTO/MMH | NTO/MMH | $O_2$/MMH | $O_2$/MMH | $O_2/C_3H_8$ | $O_2$/RP-1 | $O_2/N_2H_4$ | $O_2$/50-50 |
|---|---|---|---|---|---|---|---|---|---|---|
| Cooling Method | R/F/R | D/F/R | R/F/R | D/F/R | R/F/R | D/F/R | R/R | R/R | R/R | R/F/R |
| Chamber Pressure,psia | 125 | 125 | 125 | 125 | 100 | 100 | 100 | 100 | 100 | 100 |
| Expansion Ratio | 72 | 72 | 72 | 72 | 58 | 58 | 58 | 58 | 58 | 58 |
| Mixture Ratio | 1.6 | 1.3 | 1.65 | 1.65 | 1.2 | 1.0 | 2.6 | 2.5 | 0.8 | 1.2 |
| Delivered $I_s$, sec | 313.9 | 297.9 | 313.0 | 304.8 | 331.6 | 318.5 | 339.3 | 324.0 | 331.5 | 328.3 |
| Engine Weight, lb | 185 | 150 | 185 | 150 | 210 | 180 | 258 | 223 | 207 | 210 |
| Engine Length, in. | 73 | 70 | 73 | 71 | 74 | 72 | 77 | 86 | 77 | 72 |
| Rad. Attach $\epsilon$ | 7 | 3 | 7 | 3 | 6 | 3 | 21 | 5 | 6 | 6 |
| Extension Materia' | Cb/Ti | Cb/Ti | Cb/Ti | Cb/Ti | Cb/Ti | Cb/Ti | Ti | Cb/Ti | Cb/Ti | Cb/Ti |
| Combustor Length,in. | 11 | 8 | 11 | 9 | 12 | 10 | 15 | 24 | 15 | 10 |
| Contraction Ratio | 2 | 2 | 2 | 2 | 2 | 2 | 2 | 2 | 2 | 2 |
| Liner Material | CRES | CRES | CRES | CRES | CRES | CRES | Copper | CRES | CRES | CRES |
| Min.Channel Height,in | .062 | .025 | .062 | .025 | .068 | .025 | .160 | .250 | .145 | .071 |
| Number of Channels | 180 | 514 | 180 | 514 | 202 | 565 | 172 | 202 | 202 | 202 |
| Film Coolant Flow,pct | 2.9 | 13.5 | 2.0 | 8.4 | 2.6 | 9.4 | 0 | 0 | 0 | 2.7 |
| Sleeve Length,in. | - | 2.7 | - | 2.2 | - | 2.7 | - | - | - | - |
| Engine Inlet Pressure Ox/Fuel, psia | 169/195 | 169/177 | 169/189 | 169/177 | 138/153 | 138/138 | 138/159 | 138/144 | 138/150 | 138/156 |
| Cooling Jacket$\Delta$P,psi | 21 | 6 | 16 | 6 | 14 | 7 | 20 | 3 | 11 | 17 |
| Injector Ox $\Delta$P,psia | 23 | 23 | 23 | 23 | 18 | 18 | 23 | 23 | 18 | 18 |
| Injector Fuel $\Delta$P, psi | 27 | 30 | 27 | 30 | 18 | 18 | 23 | 23 | 18 | 18 |

R/F/R Regen/Film/Radiation
D/F/R Dump/Film/Radiation
R/R Regen/Radiation

F = 6000 lb
$D_{exit}$ = 50 in.
7 Degree Gimbal
70 Percent Nozzle

TABLE 6. OVERALL OME DESIGN POINT COMPARISON OF COOLING METHODS

| PROPELLANTS | NTO/MMH (MR=1.65) | | NTO/50-50 (MR=1.60) | | $O_2$/MMH | |
|---|---|---|---|---|---|---|
| COOLING | REGENERATIVE | FILM | REGENERATIVE | FILM | REGENERATIVE (MR=1.2) | FILM (MR=1.0) |
| $I_s$, sec | 313.1 | 304.8 | 313.9 | 297.9 | 330.9 | 318.0 |
| $\Delta W_{I_s}$, lb | Ref. | +681 | Ref. | +1312 | Ref. | +877 |
| $W_{eng}$, lb | 185 | 150 | 185 | 150 | 210 | 180 |
| $\Delta W_{eng}$, lb | Ref. | -70 | Ref. | -70 | Ref. | -60 |
| Max. $P_{in}$, psia | 189 | 177 | 195 | 177 | 153 | 138 |
| $\Delta W_{P_{in}}$, lb | Ref. | -71 | Ref. | -106 | Ref. | -105 |
| $\Sigma\Delta W$, lb | Ref. | +540 | Ref. | +1136 | Ref. | +712 |

OVERALL OME DESIGN POINT COMPARISON OF PROPELLANT COMBINATIONS

| PROPELLANTS | NTO/MMH | NTO/50-50 | $O_2$/MMH | $O_2$/50-50 | $O_2$/RP-1 |
|---|---|---|---|---|---|
| OMS Weight, lb | 27,350 | 27,300 | 27,050 | 27,240 | 27,790 |

Other factors strongly influencing the design selection were reliability, safety, maintenance, operating limits and development costs. Regenerative cooling, for example, is considered to be more reliable than film cooling due to its double-wall type construction and essentially self-healing (i.e., film cooling) capability should a crack occur in the hot-wall liner. The regeneratively cooling technique was selected for this reason in conjunction with its superior performance as compared to a film cooled design.

NTO oxidizer and amine fuels were selected over LOX and hydrocarbon fuels, respectively, due to reduced development risk, cost and schedule.

Fuel selection among the amines considered was influenced strongly by cooling safety and operating limits. Both MMH and 50-50 fuels are considerably more stable than hydrazine and are capable of higher operating temperatures without exothermic decomposition. The freezing point of MMH (-63 F) is considerably below that of 50-50 (18 F) and permits a greater range of mission duty cycles. The MMH is also somewhat more stable thermally than 50-50.

## Flight Design Selection Summary

The resulting flight configuration of the OME thrust chamber assembly (selected in conjunction with NASA/JSC) shown in Fig. 6 includes the injector, the regeneratively cooled chamber and the radiation cooled nozzle. The radiation cooled nozzle attaches at an area ratio of 7 and extends to an area ratio of 72 which corresponds to an external exit diameter of 50 inches at the 6000-pound thrust level for a chamber pressure of 125 psia. The regeneratively cooled thrust chamber used channel wall construction with an uppass coolant circuit from an area ratio of 7 to the injector and has a contraction area ratio of 2. The tapered contour from the injector to the throat favors boundary layer buildup and enhances coolant characteristics at the throat. The chamber has an integral auxiliary fuel cooling ring which contains 180 orifices using 6.4 percent of the fuel (2.4 percent of the propellants). This auxiliary film coolant lowers the fuel temperature rise and the resultant regenerative coolant jacket $\Delta P$. The regenerative coolant channels are machined into a CRES liner and closed out with electroformed nickel.

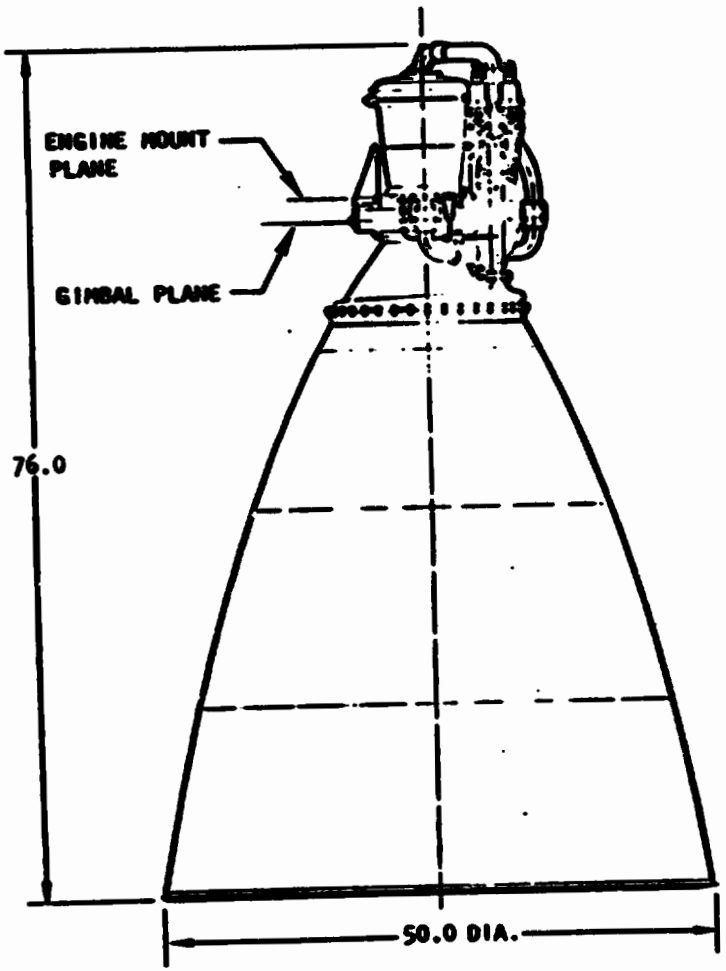


**ENGINE CHARACTERISTICS**

| | |
|---|---|
| THRUST POUNDS | 6000 |
| PROPELLANTS | $N_2O_4$/MMH |
| MIXTURE RATIO, O/F | 1.65 |
| CHAMBER PRESSURE, PSIA | 125 |
| NOZZLE AREA RATIO, | 72 |
| $I_S$, SECONDS | 313 |
| COOLING | |
| REGENERATIVE | $\epsilon = 7$ |
| FILM, % W | 2.4 |
| RADIATION | Cb/Ti SKIRT |
| VALVE TYPE | QUAD-REDUNDANT BALL VALVE |
| TVC | GIMBAL (±7 DEG) |
| COMBUSTION STABILITY | AC. CAV. |
| WEIGHT, LBS | 180 |

Figure 6. OME Thrust Chamber Assembly

## SUBSCALE REGENERATIVE COOLING EVALUATION

The use of electrically heated tubes and channels was shown to provide an economical method of obtaining valuable steady-state and transient data to assist in the design of regeneratively cooled thrust chambers. More than 300 tests were conducted to provide data on amine fuel heat flux limits, chamber hot-start capability and the ability of an amine cooled chamber to ingest helium either as discrete bubbles or in a dispersed form.

### Steady-State Burn Out Heat Flux Capability

Basic burnout data were obtained in circular CRES tubes with both MMH and 50-50 fuels. The burnout heat flux is that condition at which transition from nucleate to film boiling occurs with a resultant sharp rise in wall temperature. The wall temperature increase is normally sufficient to cause tube failure ("burn-out") unless the heat flux is rapidly reduced. The maximum heat flux is a function of coolant velocity V and subcooling $\Delta T_{Sub} (= T_{Saturation} - T_{Coolant})$.

The results of the MMH tests are presented in Fig. 7 for both Rocketdyne IR&D and contractual tests. The OME design curve utilized in the regeneratively cooled chamber designs is also shown.

The results of the asymmetrically heated rectangular channel tests are shown in Fig. 8 for MMH. The effective maximum heat flux level is less than that for the round tube due to a concentration of heat in the corner of the channel. This effect can be predicted, as shown, by use of a 2-D computer conduction model in conjunction with the basic round tube results.

### Adverse Operating Conditions

The OME may be required to start with a chamber which is hot because of soak-out from a previous firing or because of the heating effects of other engines.

In order to determine whether detonations or fouling would occur as a result of these starts, tests were conducted with electrically heated tubes. To simulate the materials of construction used in the OME thrust chamber, tubes made of electroformed nickel and CRES, the tubes were heated electrically with no propellant in the tube. The low power level required to bring the tubes to an equilibrium temperature without cooling was maintained while the coolant valve was open and coolant flowed through the tube. Coolant flowrates as low as 1/4 of the flowrate expected during start was tested at tube temperatures of up to 1600 F for both materials. No instances of detonation or fouling occurred. The results of these tests were verified, to some extent, during subsequent thrust chamber tests.

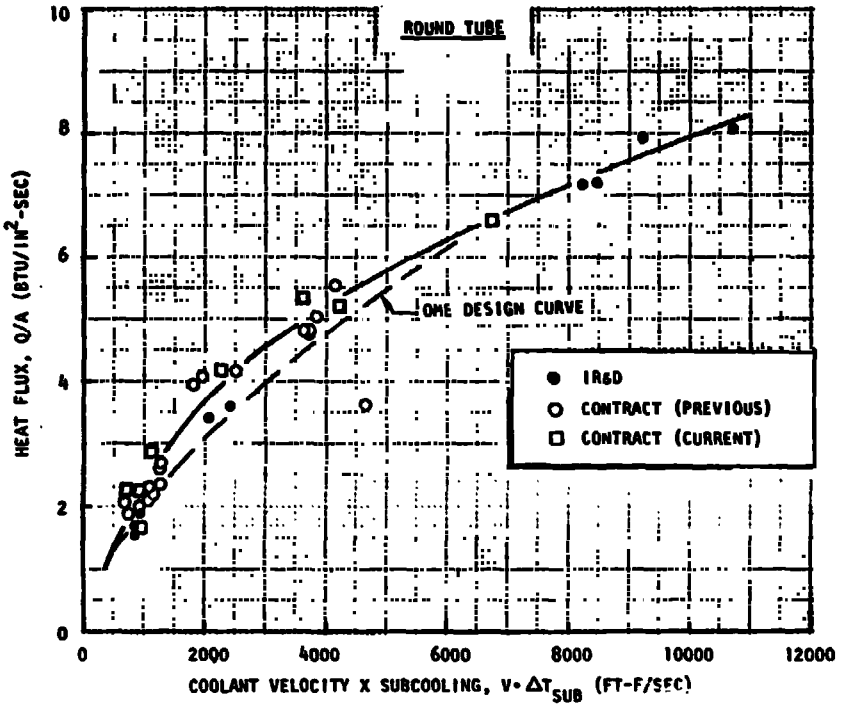


Figure 7. Experimental Burnout Heat Flux Data for MMH

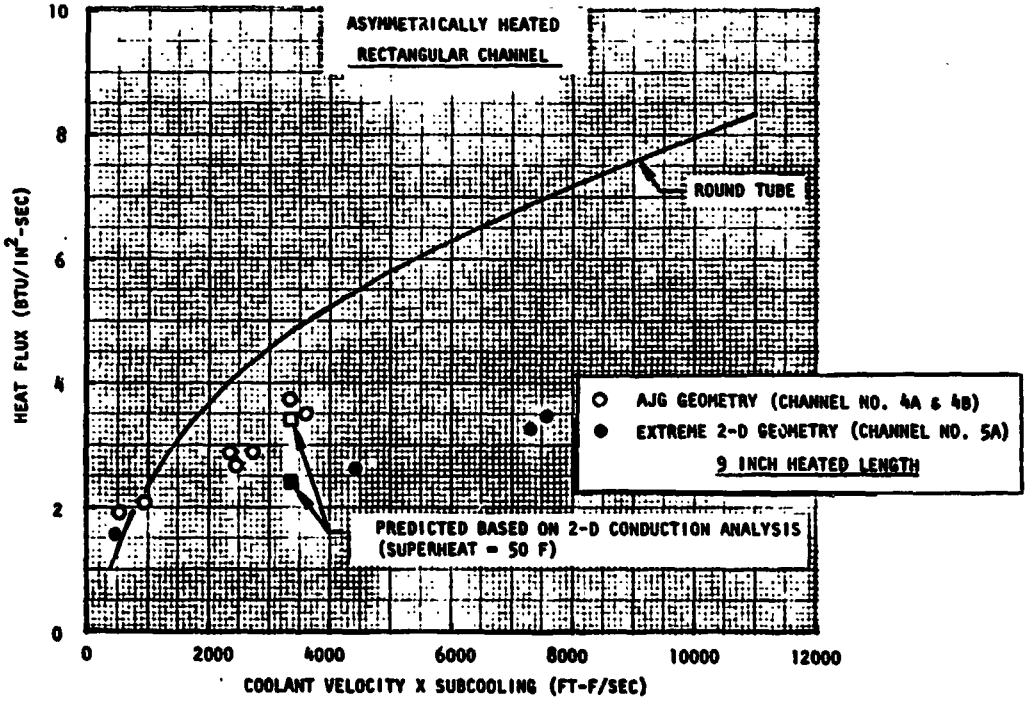


Figure 8. Experimental Burnout Heat Flux Data for MMH

Tests were conducted with a single channel to determine if large helium bubbles could be ingested into the thrust chamber without overheating. Nominal propellant flow was initiated; a nominal heat flux was electrically applied; and a bubble of known volume was passed through the heated tube and subsequently followed by a continuation of nominal coolant flow. The temperature of the heated channel wall rose while the bubble passed through the channel and decayed when the fresh coolant entered. No damage occurred to the heated channel hardware even though bubbles of durations up to 1.3 seconds were passed through the heated hardware. Since it has been calculated that a large helium bubble would reach the injector in approximately 0.3 seconds and result in a substantial reduction in the heat flux, the heated channel test data indicated that the OME thrust chamber could tolerate ingestion of a massive helium bubble. Subsequent tests with a complete thrust chamber verified these data.

Helium ingestion as a dispersed mixture (froth) could continue for a relatively long time without an appreciable decrease of the heat flux. MMH with various amounts of helium ingested in this fashion was passed through the heated channel in order to determine whether the heat flux correlation was affected significantly by the helium ingested in this manner. The test results indicate that only a slight reduction in the burnout heat flux capability results from ingestion of dispersed helium in quantities as large as 40 percent by volume.

A test series was conducted with the three-channel panel to simulate plugging of one channel on an OME thrust chamber. The center channel of the panel was plugged on the upstream side for most cases and on the downstream side for one test while nominal flow was maintained in the outer two channels. No detonations occurred with either type of plugging. The results, shown in Fig. 9 indicate a significant reduction in the flow capabilities of the adjacent channels. The data shown can be used to design chambers for this off-design condition.

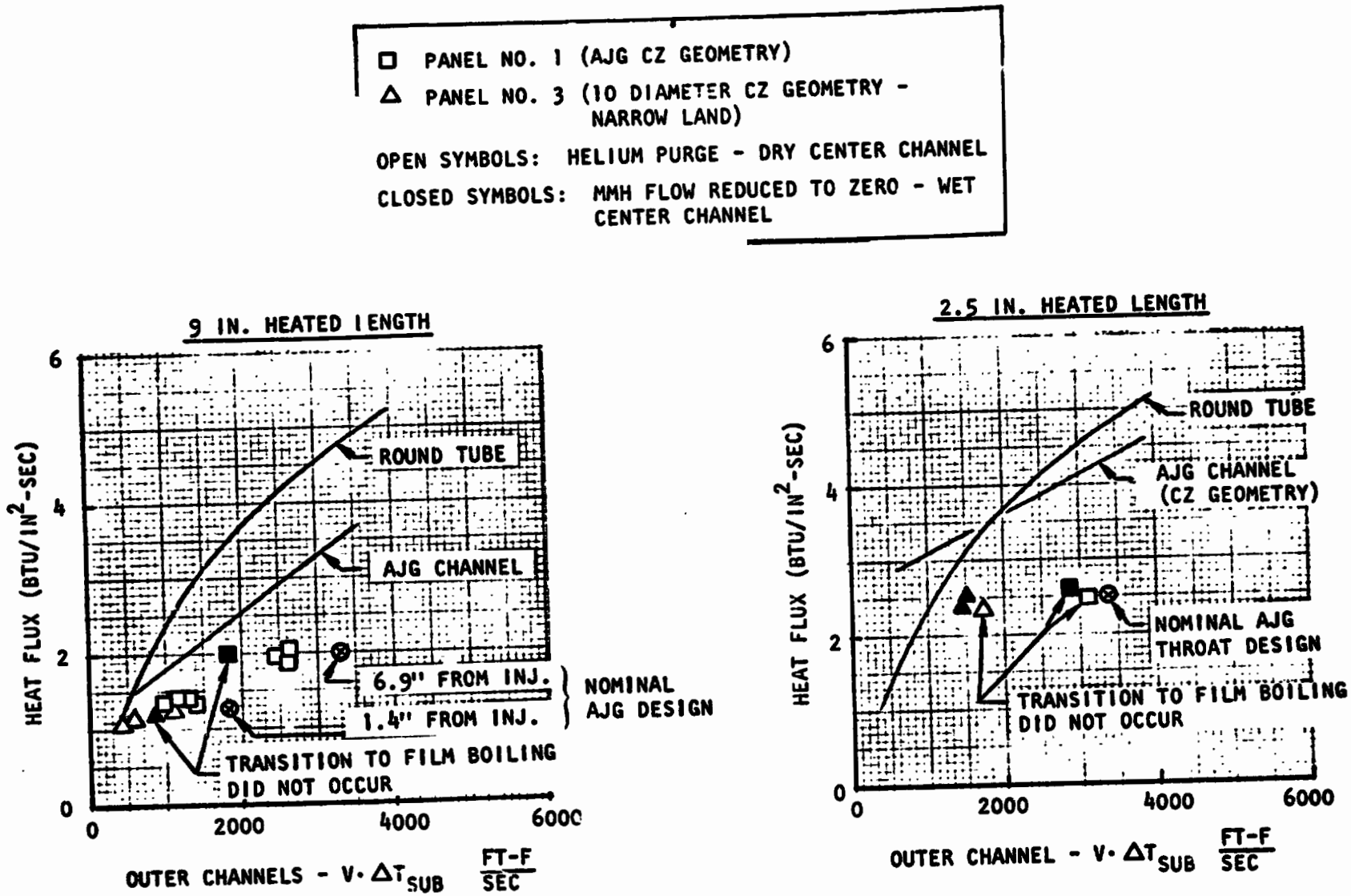


Figure 9. Effect of Completely Plugged Channel on Adjacent Channels Maximum Heat Flux Capability

## INJECTOR EVALUATION

### Subscale Injector Element Characterization

A total of 81 tests were conducted during the program. Typical test results on the like-doublet injectors are shown in Fig. 10 and 11. The optimum element configuration for hot fuel is indicated to be that which has an oxidizer-fuel spacing of 0.4 inch and a cant angle of $45^{\circ}$. For the optimum element configuration, the effects of mixture ratio, chamber pressure, and oxidizer temperature (below 100 F) are seen to be negligible. Performance was almost insensitive to fuel temperature but indicated the possibility of a slight degradation with increasing fuel temperature. The data indicated that no significant increase in performance would take place with chamber lengths greater than 10 inches so that performance was mixing limited beyond that value.

The triplet element test data also indicate an insensitivity to mixture ratio, chamber pressure, and oxidizer temperature. However, performance was more severely degraded by increasing fuel temperature than that of the like-doublet element. It appeared that the performance of the triplet element would also not increase significantly for chamber lengths greater than 10 inches.

No bombs were detonated in the chamber during these tests. However, the triplet injectors indicated low frequency (300 Hz) oscillations on almost every test. The like-doublet injectors were stable in every case with no indication of pops or oscillations.

The results of the study indicate like-doublet injectors can be designed to avoid blowapart with hot fuels. The optimum like-doublet element configuration was found to be an element with a cant angle of $60^{\circ}$ and an oxidizer-fuel separation of approximately 0.4 inch. The performance differences observed between the various subscale configurations would be substantially reduced by inter-element mixing in a full-scale injector.

### Full-Scale Injector Element Characterization

The performance test results for the L/D #1 injector are shown in Fig. 12. Performance without BLC was found to be fairly insensitive to chamber pressure, mixture ratio, or fuel temperature. The performance with BLC is approximately 1 percent lower. The performance with BLC is quite insensitive to fuel temperature, chamber pressure, or mixture ratio. The injector was tested with a combustion chamber having a smaller throat area in order to provide a contraction ratio of 3 to 1. The performance data obtained with this configuration without BLC indicates that for a fixed injector diameter, performance would be degraded by increasing the contraction ratio.

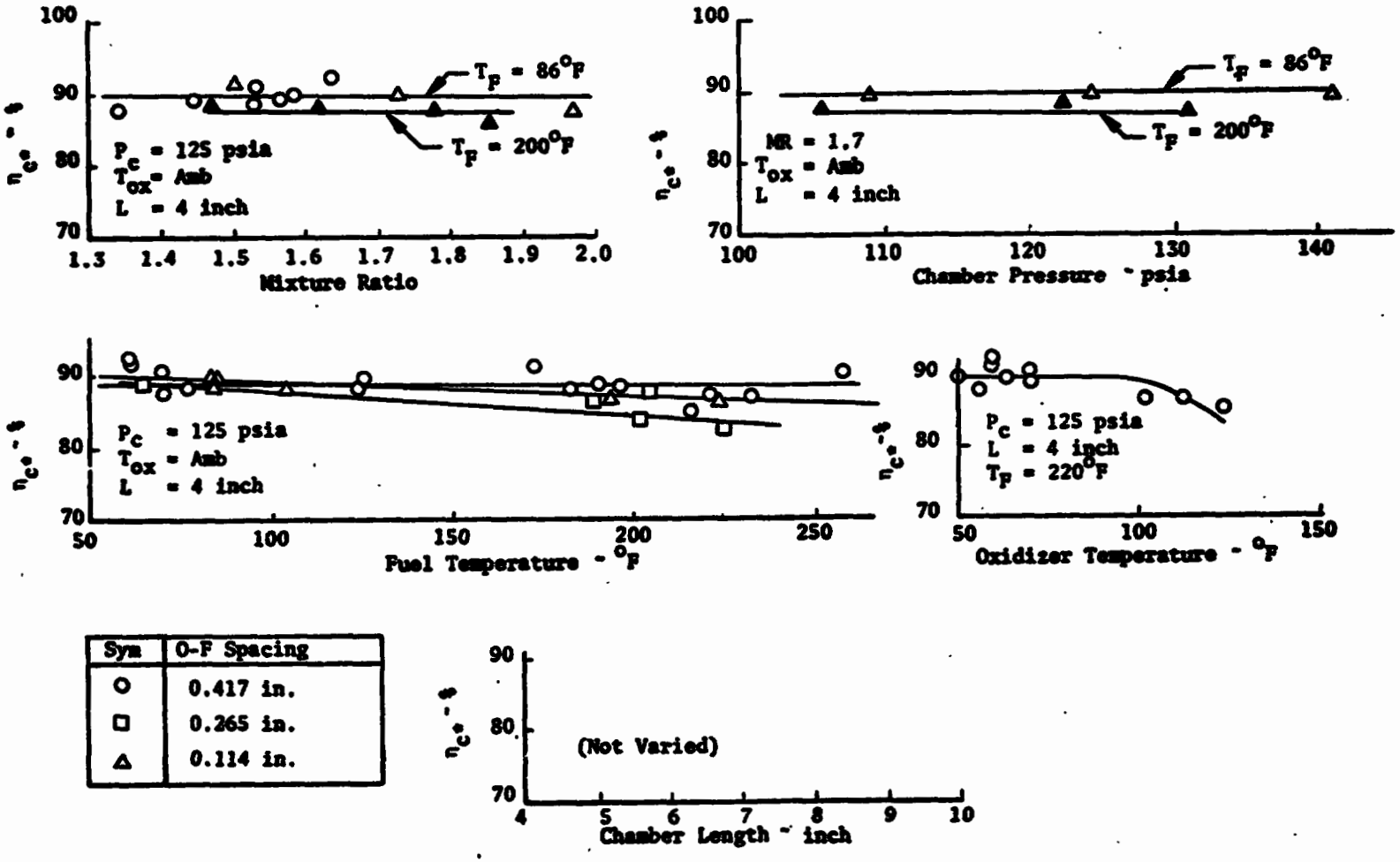


Figure 10. Summary of Experimental Results for 45 Degree Cant Angle Like-Impinging Doublet Injectors

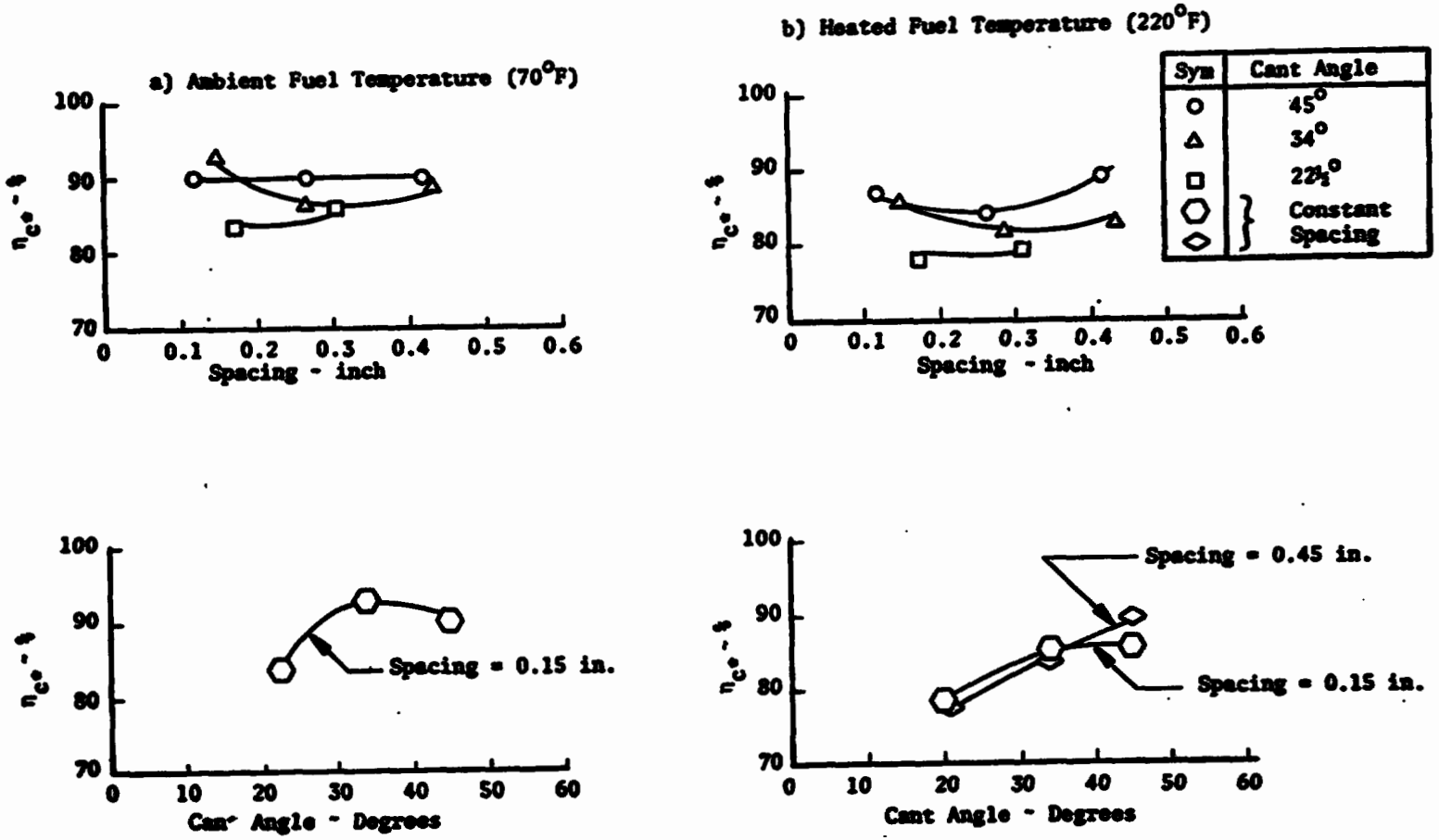


Figure 11. Effect of Cant Angle and Spacing on c* Efficiency for Like-Doublet Injector With Ambient and Heated Fuel

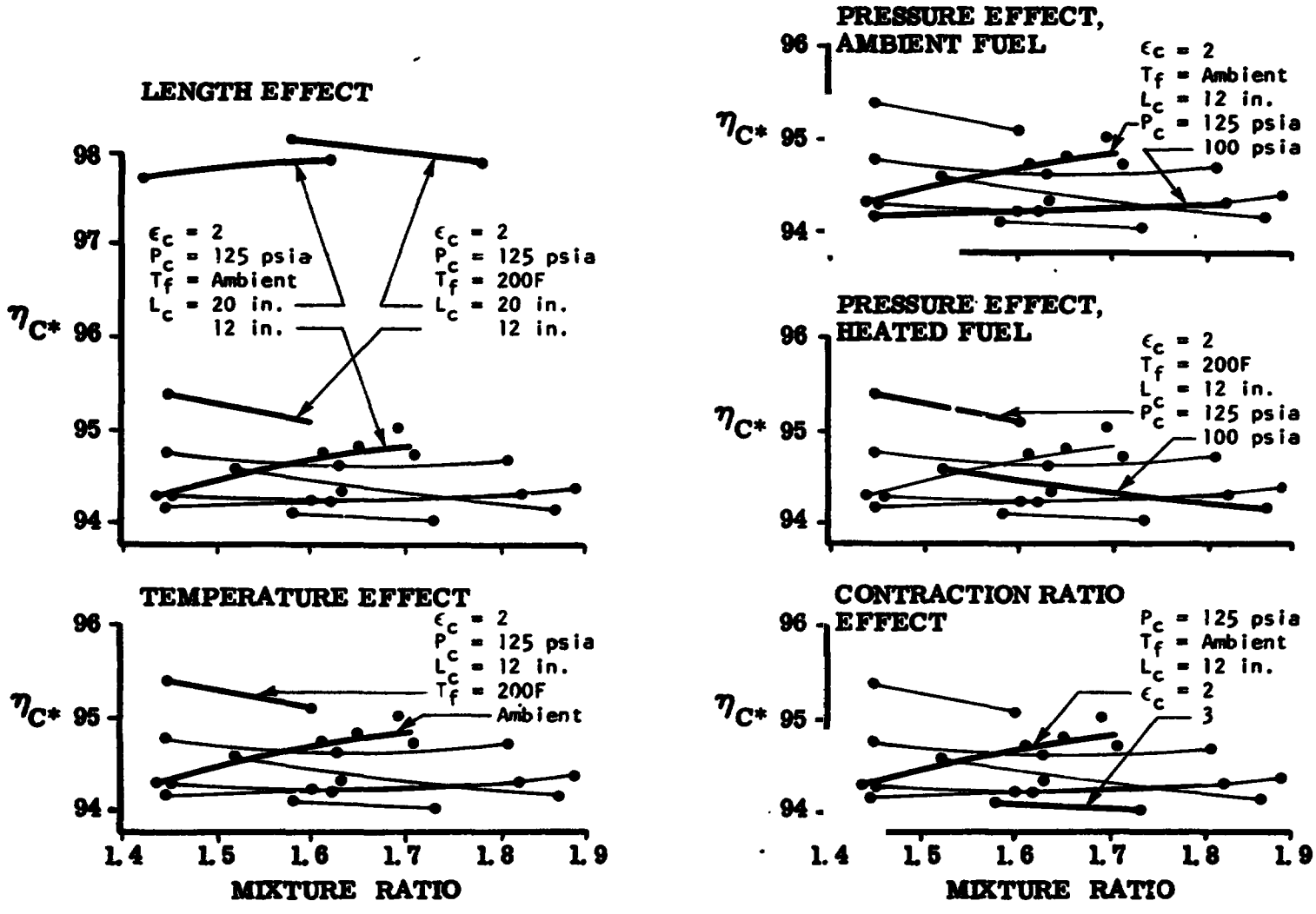


Figure 12. Like-Doublet Injector Performance - No Film Coolant

Performance of the L/D #4 injector was virtually insensitive to chamber pressure, mixture ratio, or fuel temperature. The performance of the L/D #4 injector was expected to equal or exceed that L/D #1 because of the more optimum element configuration of the former injector. However, the results indicate lower performance of the L/D #4 injector over the range of chamber lengths of interest. The lower performance of the L/D #4 was attributed to the radial sequencing of the elements or to oxidizer orifice hydraulic characteristics (the discharge coefficient of the oxidizer side of the L/D #4 was 0.66.

Another L/D element injector, L/D #2 from an IR&D program, having an 8-inch diameter was tested in solid wall hardware. This injector had more elements and modified element characteristics relative to L/D #1. The performance and the heat flux profile of the L/D #2 injector were similar to that of L/D #1. The L/D #2 injector was used primarily on Contract NAS9-12524.

The heat flux data taken on the L/D #1 injector indicated a heat flux value at the throat approximately 3 Btu/in$^2$-sec without BLC, which reduced to 2.4 Btu/in$^2$-sec by the addition of 2.5 percent BLC. The heat flux in the cylindrical portion of the chamber was approximately 2.5 and 1.6 Btu/in$^2$-sec without and with the BLC respectively.

Full-Scale Stability Characterization

Stability data were obtained for several injector/chamber/cavity configurations. Tests were conducted on both 8- and 10-inch like-doublet injectors. The acoustic cavities for these tests were located in a single row around the injector face, 12 equal area cavities separated by partitions. Four of the cavities (equally spaced) were turned to suppress the third tangential and first radial modes of instability. The remaining eight cavities were turned to suppress the first tangential mode of stability.- Test results are summarized in Tables 7 and 8. Results from testing the 8.2-inch diameter (low contraction ratio) chamber show that:

1. Stability was readily achieved with a contoured entrance cavity without overlap (see sketch).

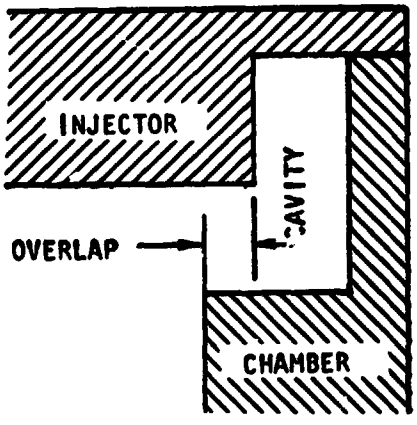


R-9686-1

## TABLE 7. SUMMARY OF STABILITY RESULTS FROM LOW CONTRACTION RATIO CHAMBER TESTS

| Objective | Primary Cavity (1) σ | Primary Cavity (2) $\ell_e$, in. | Secondary Cavity (1) σ | Secondary Cavity (2) $\ell_e$, in. | $P_c$, psia | Overall Mixture Ratio | Fuel Inj. Temp., F | Maximum Damp Time, msec | Frequency, Hz | Stability |
|---|---|---|---|---|---|---|---|---|---|---|
| Stability of Basic Configuration | 0.148 | 1.60 | 0.074 | 0.78 | 130 | 1.80 | 180 | 14 | 2330 | Stable |
| | | | | | 126 | 1.71 | 190 | 220 | 2550 | Unstable |
| | | | | | 125 | 1.69 | 160 | 70 | 2570 | Unstable |
| | | | | | 140 | 1.55 | 165 | 11 | 2300 | Stable |
| | | | | | 113 | 1.52 | 165 | 11 | | |
| | | | | | 111 | 1.79 | 175 | 12 | | |
| Evaluate Effect of Manifold Dams | | | | | 137 | 1.52 | 175 | 12 | | Stable |
| | | | | | 123 | 1.66 | 160 | 13 | | |
| | | | | | 141 | 1.86 | 165 | 15 | | |
| | | | | | 111 | 1.42 | 150 | 14 | | |
| Stability with Reduced Open Area | 0.12 | 1.58 | 0.06 | 0.76 | 136 | 1.44 | 220 | 11 | | Stable |
| | | | | | 127 | 1.68 | 205 | 12 | 2770 | |
| | | | | | 140 | 1.80 | 195 | 70 | 2790 | Unstable |
| | | | | | 111 | 1.45 | 190 | 10 | | Stable |
| | | | | | 111 | 1.84 | 175 | 21 | 2790 | Marginal |
| | | | | | 127 | 1.61 | 175 | 10 | 2770 | Stable |
| | | | | | 143 | 1.65 | 170 | 18 | 2750 | |
| | | | | | 128 | 1.69 | 160 | 11 | 2800 | |

(1) σ = fractional open area based on injector face area

(2) $\ell_e$ = effective cavity depth

## TABLE 8. SUMMARY OF STABILITY RESULTS FROM HIGH CONTRACTION RATIO CHAMBER TESTS

| Objective | Primary Cavity (1) σ | Primary Cavity (2) $\ell_e$, in. | Secondary Cavity (1) σ | Secondary Cavity (2) $\ell_e$, in. | $P_c$, psia | Overall Mixture Ratio | Fuel Inj. Temp., F | Maximum Damp Time, msec | Frequency, Hz | Stability |
|---|---|---|---|---|---|---|---|---|---|---|
| Search for Minimum Open Area | 0.099 | 2.08 | 0.069 | 0.98 | 120 | 1.64 | 190 | 7 | | Stable |
| | | | | | 134 | 1.84 | 220 | 7 | | |
| | | | | | 136 | 1.54 | 210 | 6 | | |
| | | | | | 118 | 1.73 | 160 | 9 | | |
| Search for Minimum Depth | 0.148 | 1.28 | | | 127 | 1.66 | 190 | 570 | 2640 | Unstable |
| Confirm Stability at Nominal Depth | 0.148 | 2.12 | | | 126 | 1.66 | 201 | 6 | | Stable |
| | | | | | 140 | 1.80 | 192 | 6 | | |
| | | | | | 132 | 1.44 | 188 | 6 | | |
| | | | | | 114 | 1.82 | 189 | 7 | | |
| | | | | | 126 | 1.62 | 190 | 6 | | |
| | | | | | 140 | 1.61 | 185 | 5 | | |
| | | | | | 110 | 1.48 | 176 | 7 | | |
| | | | | | 126 | 1.67 | 187 | 8 | | |
| | | | | | - | - | - | 8 | | |
| | | | | | 125 | 1.62 | 70 | 8 | | |
| | | | | | 139 | 1.85 | 68 | 7 | | |
| Confirm Stability with Long Chamber | 0.099 | 2.08 | | | 129 | 1.42 | 65 | 7 | | |
| | | | | | 125 | 1.69 | 225 | 8 | | |
| | | | | | 140 | 1.85 | 200 | 7 | | |
| | | | | | 140 | 1.54 | 194 | 7 | | |
| | | | | | 112 | 1.88 | 183 | 8 | | |
| | | | | | 112 | 1.71 | 194 | 8 | | |
| | | | | | 126 | 1.66 | 183 | 8 | | |

(1) σ = Fractional open area based on injector face area

(2) $\ell_e$ = Effective cavity depth

2. Stability was dominated by 2300 to 2800 Hz oscillation and which was improved by installing baffles (dams) in the fuel manifold.

3. The change in BLC introduction from a separate downstream injector to the periphery of the main injector did not significantly affect stability. Moreover, the stability of the L/D #1 injector appeared comparable but slightly better than that of the L/D #2 injector.

The 2300 to 2900 Hz instability data may be grouped into three sets:

1. Stability was achieved with the proper cavity open area. A 2300 Hz oscillation appeared briefly during the decay transient after two bombs. The phase angles suggest a first tangential angular distribution of pressure.

2. Two sustained instabilities occurred with frequencies near 2560 Hz. The amplitude and phase data suggest a precessing and then standing first tangential type pressure distribution. The pressure node appeared to stand along the fuel inlet line. The amplitudes were 35 to 70 psi peak-to-peak.

3. After installation of the manifold dams, multiple occurrences of a 2790 Hz oscillation were encountered. In each case the oscillation damped in 10 to 70 milliseconds. The amplitude and phase behavior usggested, as with the 2560 Hz oscillation, that the mode precessed initially and then stood with the pressure node along the fuel inlet. Amplitudes were 50 to 150 psi peak-to-peak.

Results from testing the 10-inch diameter (high contraction ratio) chamber show that:

1. Adequate stability was readily stable. Because the performance was somewhat low, the greater stability may not be due to the higher contraction ratio.

Acoustic Model Stability Characterization

Two kinds of acoustic model tests were made, one with relatively detailed models of the acoustic cavities only and the second with a model of the combustion chamber containing acoustic cavities. The tests with the detailed cavity models were made to measure the effective acoustic depth of these cavities associated with the entrance region. The tests with the chamber model were made to measure the influence of the cavities on the

acoustic modes of the chamber. Each kind of model was excited with an acoustic driver and the model response was measured with a microphone. The frequencies corresponding to maximum microphone response were interpreted as the resonant frequencies of the models.

Two significant observations may be made from the test results. First, the test results indicate the resonant frequency of the resonator is substantially unaffected by the position of the downstream portion of the cavity entrance, when varied over a range of 0.6 to 2.7 times the cavity width. Secondly, the overlap (0.2 inch) used with 1/4 circle entrance (similar to Aerojet partial contours) has apparently increased the effective depth by an amount approximately equal to the overlap; a conclusion inferred from comparison with the results for the rectangular entrance.

## Analysis and Interpretation of Stability Test Results

The purpose of the analytical effort under this program were to aid design of the cavities to be tested and to aid evaluation, from the available data, of the effectiveness of acoustic cavities for suppressing instabilities. Most of the effort was directed toward assessing the significance of the 2300 to 2800 Hz oscillation experienced during testing on this and other programs.

The 2300 to 2800 Hz oscillation has been encountered repeatedly during testing of 8-inch diameter chambers at Rocketdyne and Aerojet. Rocketdyne has interpreted this oscillation as not being due to a normal chamber mode and probably associated with the acoustics of the feed system. With this interpretation, the acoustic cavity would be expected to weakly affect stability. Conversely, Aerojet has interpreted with oscillation as being due to the first tangential mode of the chamber with its frequency being suppressed by the acoustic cavity. Aerojet has tried many cavity configurations in an effort to suppress the oscillation. In an effort to identify the mode or modes and clarify the implications relative to cavity effectiveness, analytical studies were made of both of these possibilities.

Results from the analysis effort do not permit the mode or modes of oscillation to be identified fully. However, it appears very unlikely that this oscillation is caused by cavity effects alone. Nevertheless, the oscillation is influenced by the cavity entrance configuration. This oscillation is also influenced by dams in the fuel manifold and, in addition, it appears to have a first tangential type of pressure distribution with the nodal position influenced by the fuel inlet position. These results suggest that the oscillation is associated with an interaction between the fuel injection system and cavity effects. The cavity influence may result from interaction between the oscillatory jet emerging from the cavity and the injection/combustion processes of adjacent injection elements.

The available test data suggest that this mode has not occurred in the 10-inch diameter chambers.

## DEMONSTRATION THRUST CHAMBER

The demonstration thrust chamber was designed to provide flexibility in testing in order to characterize the effects of BLC and coolant flowrate on chamber operating temperature and performance. The bolted test assembly included a separate film coolant ring and a short ($7 < \varepsilon < 9$) columbium nozzle. This latter item allowed investigation of nozzle radiation equilibrium temperatures and soakback characteristics.

The chamber was tested over a wide range of conditions as shown graphically in Fig. 13 . Chamber pressures ranged from 100 psi to about 180 psi and mixture ratios from 1.4 to 1.9. A total of 112 tests was conducted at both Rocketdyne (CTL-IV) and White Sands Test Facilities for a cumulative duration of 1042 seconds. Both MMH and 50-50 fuels were investigated during the test program. Testing was accomplished with two like-doublet injectors denoted as L/D #1 or L/D #2.

### Stability Characteristics

No high or low frequency instability was recorded over the entire range of chamber pressures and mixture ratios test (no bomb tests) with either MMH or 50-50 fuels with either the L/D #1 or L/D #2 injector. All configurations relied on acoustic cavities without baffles to maintain stable operation. Axial accelerometers installed on the engine thrust mount typically showed disturbances of 10-20 g's RMS at start and no significant activity during the tests.

### Performance Characteristics

Performance versus mixture ratio data was obtained with unsaturated NTO and MMH using the L/D #1 injector at CTL-IV and WSTF. Performance on the tests at nominal conditions with 2 percent auxiliary film coolant at CTL-IV and averaged approximately 310 seconds. A one percent improvement in injector performance is predicted with minimum development. Performance measured at WSTF was slightly over 308 seconds at nominal conditions. The deformed nozzle (as a result of the CTL-IV malfunction) may have resulted in a slight performance degradation at WSTF.

The variation of performance with chamber pressure and mixture ratio measured at WSTF over the ranges for which the demonstrator was designed is shown in Fig. 14 for unsaturated propellants and approximately 2 percent film cooling. An increase in performance of approximately 1-second occurs at the upper end of the nominal operating range of the OME ($P_c$ = 140 psia, o/f = 1.8), compared to performance at nominal conditions. Performance decreases by approximately 3 seconds operating at a chamber pressure of 110 psi and a mixture ratio of 1.45.

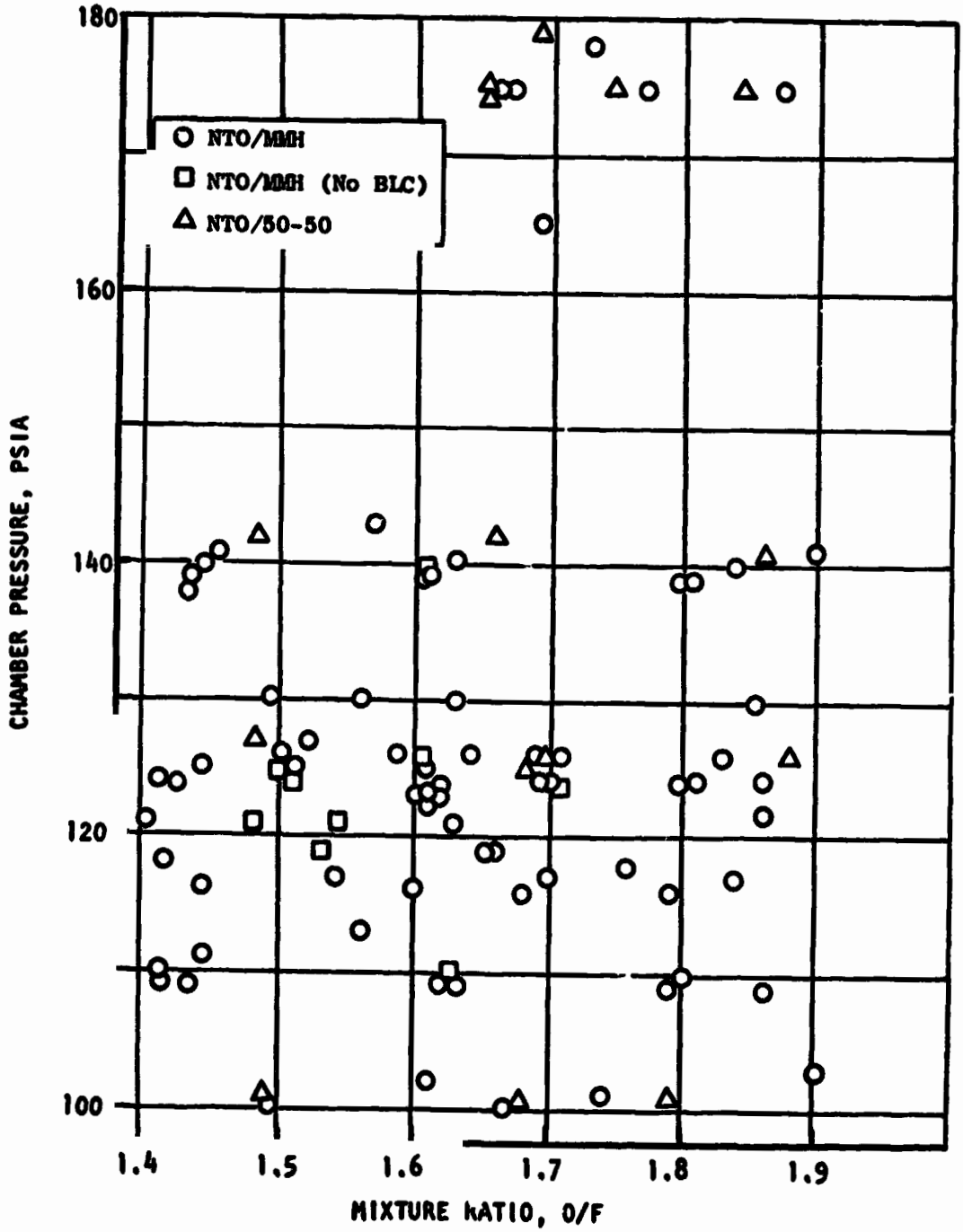


Figure 13. Demonstrator OME Thrust Chamber Operating Conditions

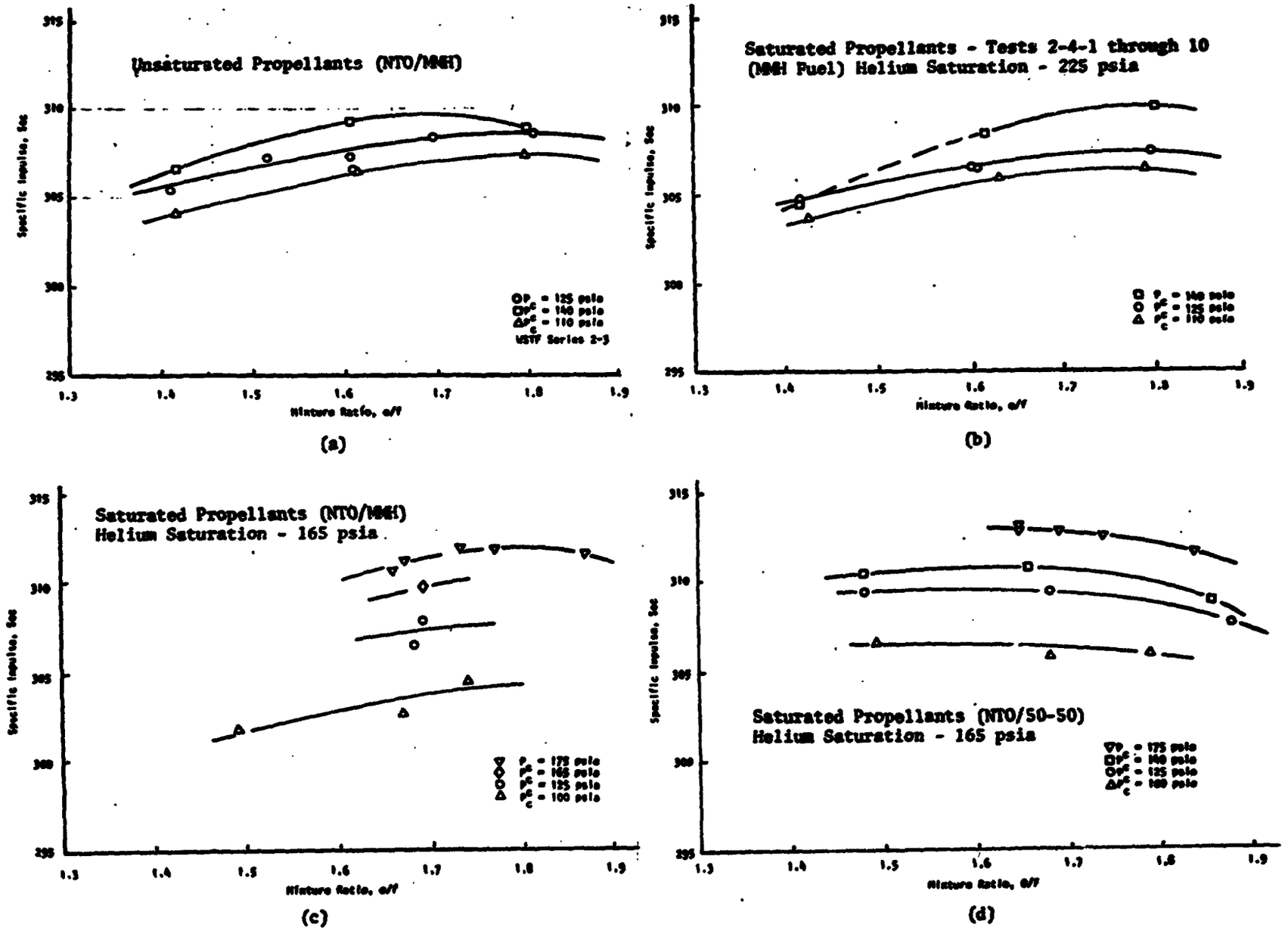


Figure 14. OME Engine Performance

Performance data measured at CTL-IV at off-design chamber pressure did not show the trend. Low pressure data were invalid due to nozzle separation. High pressure data indicated a slight performance loss.

Performance with helium saturated propellants is shown in Fig. 14b and 14c. A performance penalty of approximately 1-second results under nominal operating conditions. The shape of the measured performance curve at 140 psia chamber pressure and 225 psia saturation pressure appears to be more sensitive to mixture ratio compared to the rest of the data. However, the point at nominal mixture ratio is consistent with all other data.

Operating at a chamber pressure of 175 psia would increase the performance by about 4 seconds. An OME derivative used for a Space Tug application would operate at a chamber pressure of approximately 240 psia and would have a significantly higher area ratio. The 100 psia test conditions simulate the effect of vehicle pressurization system failure. A performance loss of over 1 percent occurs under these conditions relative to performance at the design point.

The performance of NTO with helium saturated 50-50 fuel and the #1 like-doublet injector is shown in Fig. 14d. The nominal mixture ratio for this propellant combination is 1.60 for equal tank volumes. At this mixture ratio and a chamber pressure of 125 psia, a performance level of approximately 310 seconds was measured. These tests were of 7 seconds duration. Operating at a high mixture ratio with this propellant combination results in a performance loss (rather than a performance gain as was the case with NTO/MMH) as predicted analytically. A gain of approximately 1 second in performance occurs at a chamber pressure of 140 psia. Performance sensitivity to chamber pressures is approximately the same as with the NTO/MMH combination.

## Thermal Characteristics

Heat Load. A primary consideration in terms of regeneratively cooled chambers is total heat load and coolant bulk temperature rise. A summary of the demonstration chamber heat load data as obtained at CTL and WSTF is presented in Fig. 15. It is apparent that the heat load with 2 percent BLC is considerably below the original predicted value. This result is due primarily to lower than predicted heat loads without film coolant. The like doublet injector apparently provides a cool outer core with reduced heat loads to the film coolant and chamber.

The reduced heat load results in a nominal coolant bulk temperature rise of about 135 F rather than the 175 F value utilized in the original design. A reevaluation of the minimum coolant safety factor for the demonstration chamber is given in Table 9. Based on a 1-D analysis the demonstrator is capable of satisfactory operation without BLC at off-design conditions. Two-dimensional thermal analysis would indicate a reduced factor of safety which would limit operation without BLC to close to nominal conditions.

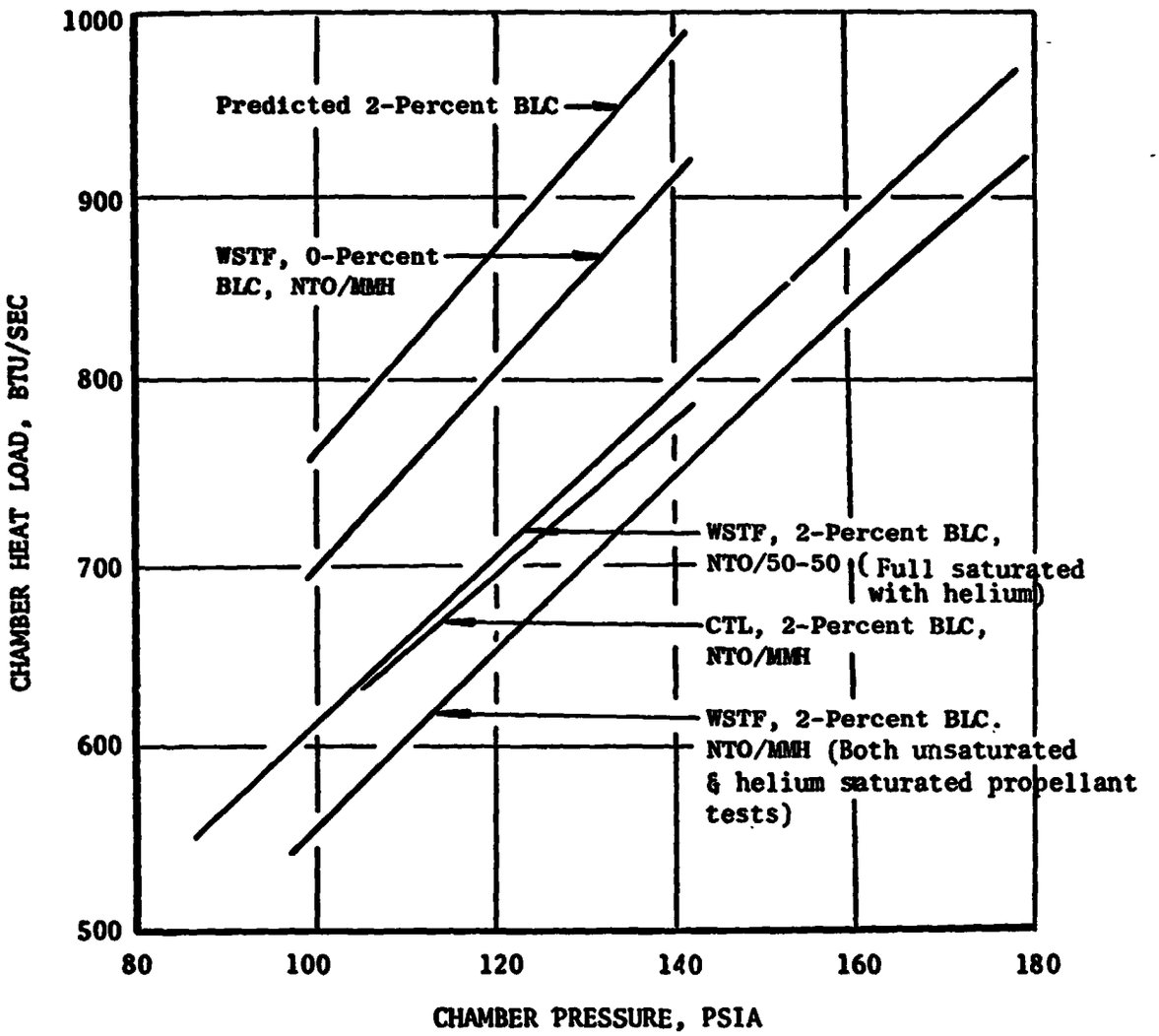


Figure 15. Summary of Demonstrator Head Load Data

TABLE 9 . THERMAL SAFETY FACTORS BASED ON EXPERIMENTAL DATA

| Propellant | Safety Factor (1-D) Nominal | Off-Design** |
|---|---|---|
| NTO/MMH with 2% BLC | 3.5 | 2.8 |
| NTO/MMH with no BLC | 2.0 | 1.4 |
| NTO/50-50 with 2% BLC | 3.0 | 2.2 |

* $P_c$ = 125 psia; $T_{bulk\ in}$ = 70 F; o/f = 1.65 (MMH), 1.60 (50-50); Fuel Injector $\Delta P$ = 45 psi

** $P_c$ = 120 psia; $T_{bulk\ in}$ = 100 F; o/f = 1.84 (MMH), 1.79 (50-50); Fuel Injector $\Delta P$ = 36 psi

Back Wall Temperatures. Back wall temperatures were measured on the thrust chamber to indicate steady-state values during operation and also values at restart. The steady-state temperature profiles were also used to indicate the coolant temperature rise profile and heat flux circumferential uniformity.

The back-wall temperatures agreed favorably with the total reduced heat load. The temperature profile indicated that the BLC was most effective in the head-end region as would be predicted. Maximum steady-state outer wall temperatures were less than 300 F. Restart at chamber temperatures approaching 500 F were accomplished without incident.

Radiation Nozzle. Limited experimental data on steady-state operation of the short Columbium radiation nozzle extension exists since nearly 30 seconds test duration is required to achieve equilibrium temperatures. A single 30-second test at CTL-IV with NTO/MMH indicated a maximum steady-state temperature of about 1900 F. A similar test at WSTF with NTO/50-50 propellants indicate maximum nozzle temperature of about 1600 F.

The predicted nozzle temperature of about 2200-2300 F for the short extension is considerably higher than the experimental values. It appears that film cooling carryover downstream of the throat results in significant reduction of the radiation nozzle temperature. This is an important result since it permits the use of a more conventional nozzle extension material with possibly significant cost savings.

## INTEGRATED THRUST CHAMBER

### Design Configuration

The Integrated Thrust Chamber (ITC) was designed, fabricated, and tested in order to obtain more extensive data on the limits of operation of a reusable chamber for OME application. The ITC differs from the demonstrator chamber primarily in the head-end region as noted previously with the film coolant being supplied from the primary injector. The ITC internal contour from injector to nozzle exit is essentially unchanged. The acoustic cavities and dams are regeneratively cooled. Channel geometry was optimized to a greater extent for the ITC based on more recent MMH 2-D cooling data in channels as obtained under this contract. The resulting design consisted of 120 channels of constant width = 0.114 inch. Inlet manifolding is simple non-flight-type as used in the demonstrator chamber.

### Test Results

The ITC was tested 156 times, in two phases, at White Sands Test Facility, for a cumulative duration of 1190 seconds. Phase I tests were concerned primarily with the steady-state stability, thermal, and performance characteristics of the ITC with additional limited tests to determine transient characteristics. These tests utilized a full 72:1 area ratio heat sink nozzle (Fig. 16 ). During Phase II, the start, shutdown, and restart characteristics of the ITC were investigated. Performance and thermal conditions for blowdown operation and for operation without film cooling were also experimentally evaluated during Phase II.

Performance Characteristics. The variation of specific impulse with chamber pressure and mixture ratio is shown in Fig. 17 for both saturated and unsaturated propellants (both fuel and oxidizer saturated with helium at 225 psia). Performance peaks at a mixture ratio of approximately 1.8 and increases with chamber pressure. The effect of saturation on performance is negligible.

A comparison with the data curve from the demonstrator tests is also shown in this figure and indicates 1 to 2 seconds lower performance at the higher mixture ratios. The data shown for the demonstrator were based upon analytical extrapolation to $\epsilon = 72$ of data taken with a 9:1 expansion area ratio nozzle. The good agreement affirms the validity of the analytical extrapolations.

Tests conducted without BLC (by plugging injector orifices) indicated a performance gain of 1.5 seconds at nominal chamber pressure and mixture ratio after adjusting for the lower fuel inlet temperature (40 F) utilized to insure safe operation.

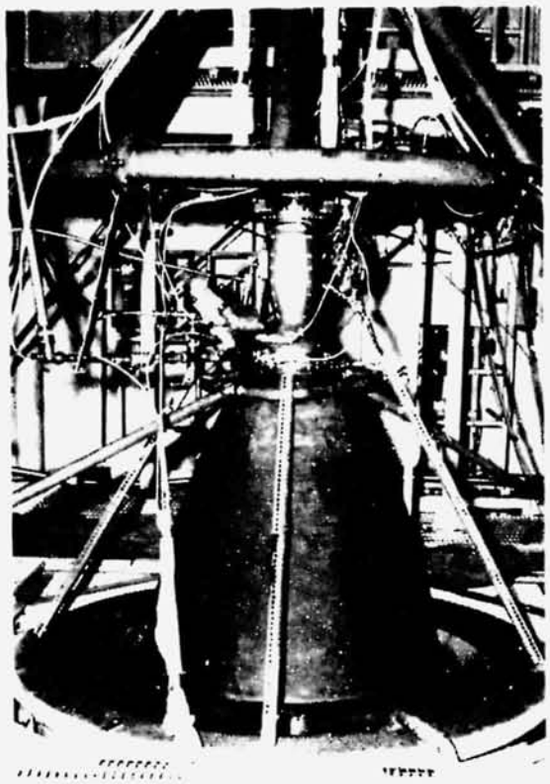

Figure 16. Integrated Thrust Chamber Engine Installation

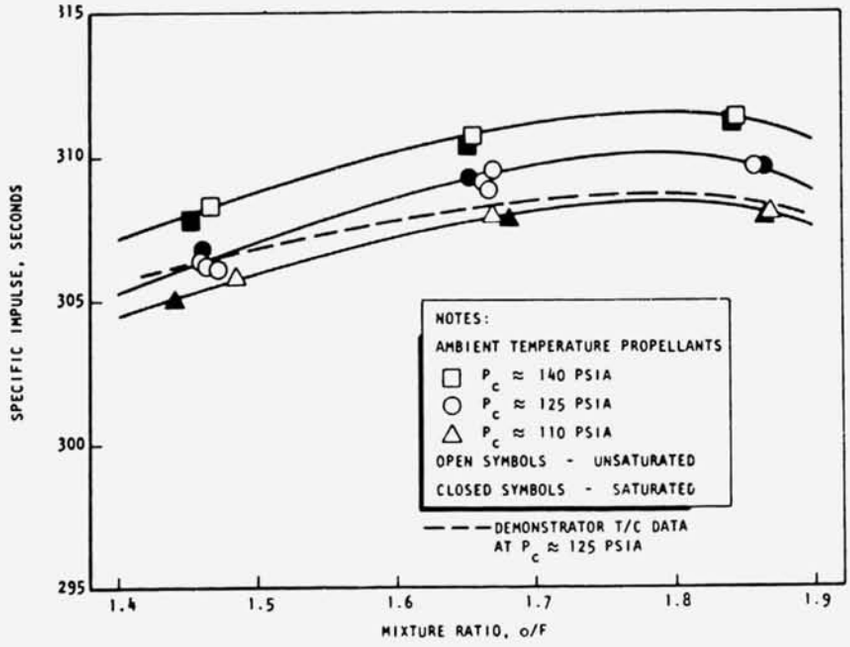


Figure 17. Integrated Chamber Performance With Ambient Temperature Propellants

Injector and coolant jacket pressure drops were experimentally determined and were in good agreement with predictions. The resulting pressure drop summary is shown in Fig. 18 .

Thermal Characteristics. Fuel temperature rise, chamber back wall temperature profiles and nozzle temperatures were measured and total heat loads calculated for all tests. The heat loads for the ITC using ambient temperature propellants (both saturated and unsaturated) are shown in Fig. as a function of chamber pressure and mixture ratio. These data follow the predicted 0.8 power of $P_c$ variation. The effect of mixture ratio and helium saturation on heat load appears negligible.

The best fit line of the demonstrator heat load results is also shown in Fig. 19 for comparison with ITC heat loads. The ITC heat loads are about 12 percent higher due primarily to the less efficient, but much simpler, method of film coolant injection employed in the ITC design. Part of the higher heat load (about one-third) results from regenerative cooling of the acoustic cavity region.

Hot propellants ( $\approx$ 100 F) did not appreciably affect chamber heat load.

The effect of eliminating BLC on ITC heat load is shown in Fig. 20 . The nominal BLC reduces the heat load by about 22 percent. Most of this reduction occurs in the cylindrical section of the chamber as determined by the back wall temperature measurements.

Nozzle Extension. Data taken on the $\epsilon$ = 72 steel heat sink nozzle and the short columbium nozzle indicate a maximum radiation equilibrium temperature of 1630 F and 1800 F with and without BLC, respectively. These results indicate that the use of a refractory material is unnecessary. The use of an L-605 nozzle extension appears feasible.

Throttling Characteristics. Discrete 5-second tests were conducted at decreasing chamber pressures with cold (40 F) unsaturated propellants. Chugging ( $\approx$ 300 Hz) was initially noted at a chamber pressure of 84 psia and occurred for about 0.6 seconds. As the chamber pressure was decreased the duration of chugging increased until at a chamber pressure of 68 psia chugging continued throughout the test. The chugging did not appear to be detrimental to the engine over the several 5-second duration tests conducted in the program. Measured heat loads were comparable to steady-state values extrapolated to the lower pressures. Based on these tests it appears the chamber can be started at pressures as low as approximately 90 psia without chugging. During blowdown operation the chamber may be throttled to about 65 to 75 psia without chugging.

Start and Shutdown Characteristics. The ITC was subjected to extensive start, shutdown, and restart testing using facility and engine ducting configured to simulate, as far as possible, the volumes and lengths of the current OMS propellant feed system. These tests are discussed in detail in the Final Report and the appropriate test reports as listed in Table 1 .

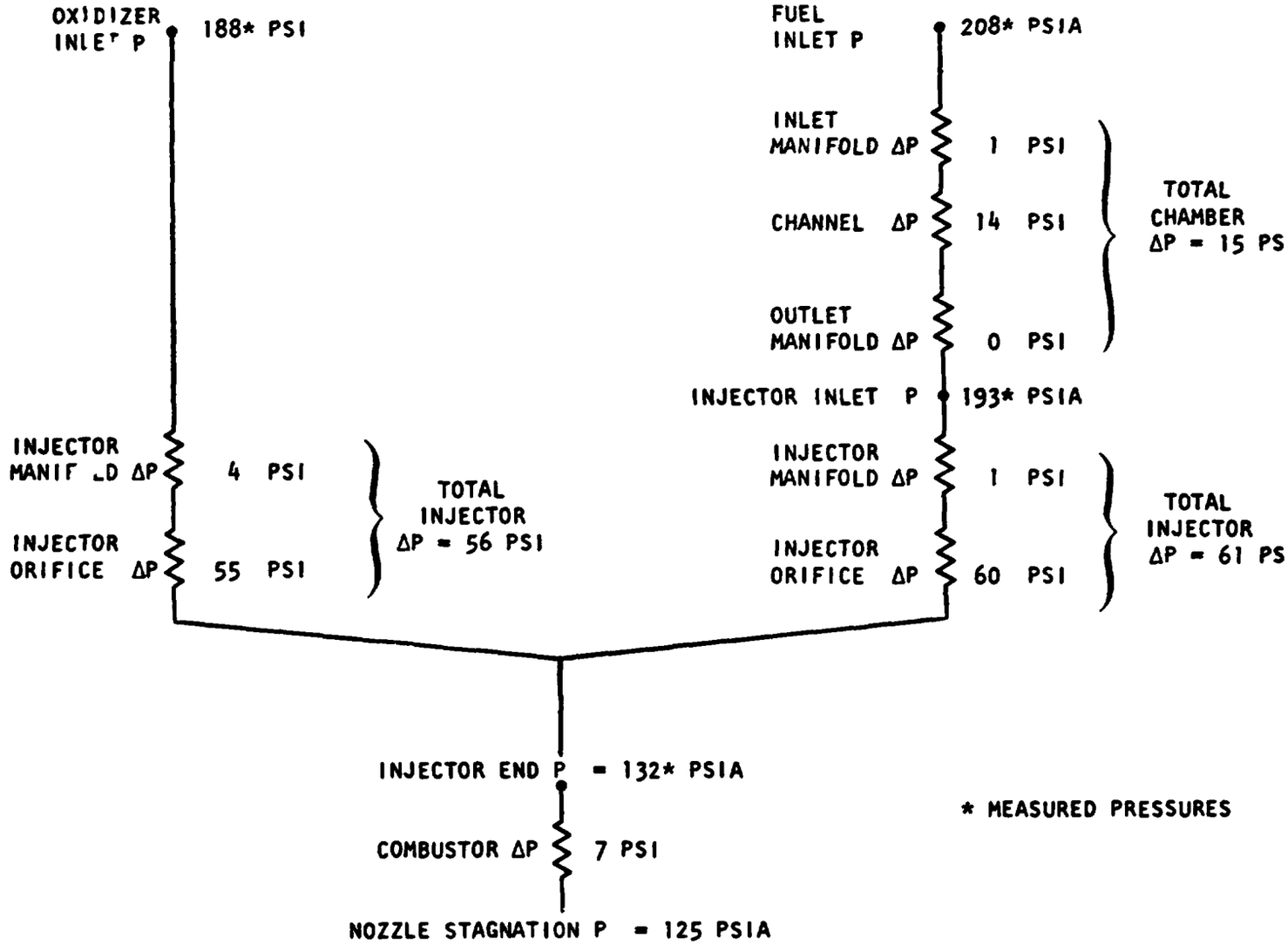


Figure 18. Integrated Thrust Chamber Assembly Pressure Drops

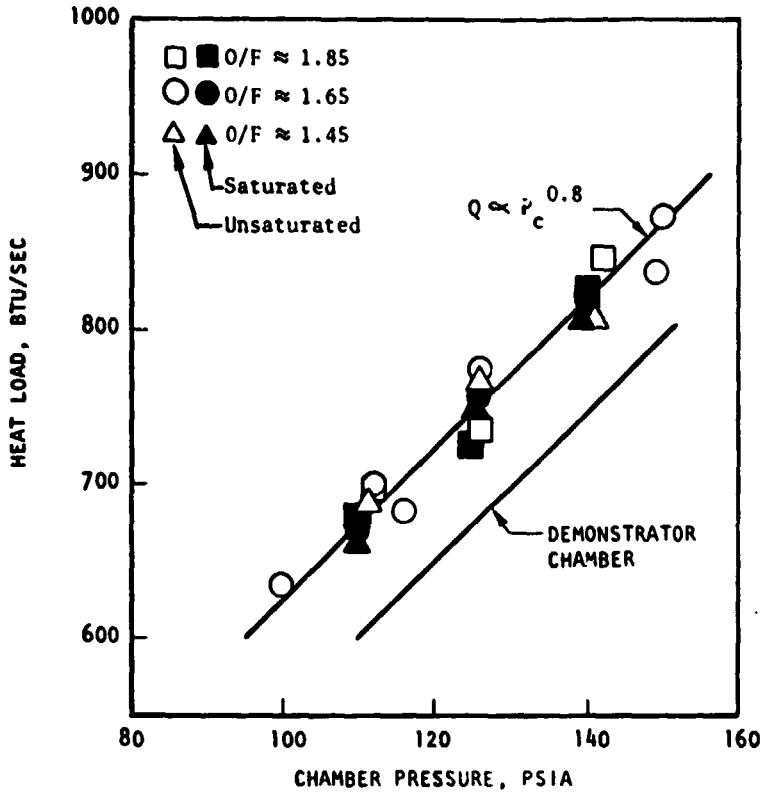


Figure 19. Integrated Chamber Heat Load with Ambient Propellants

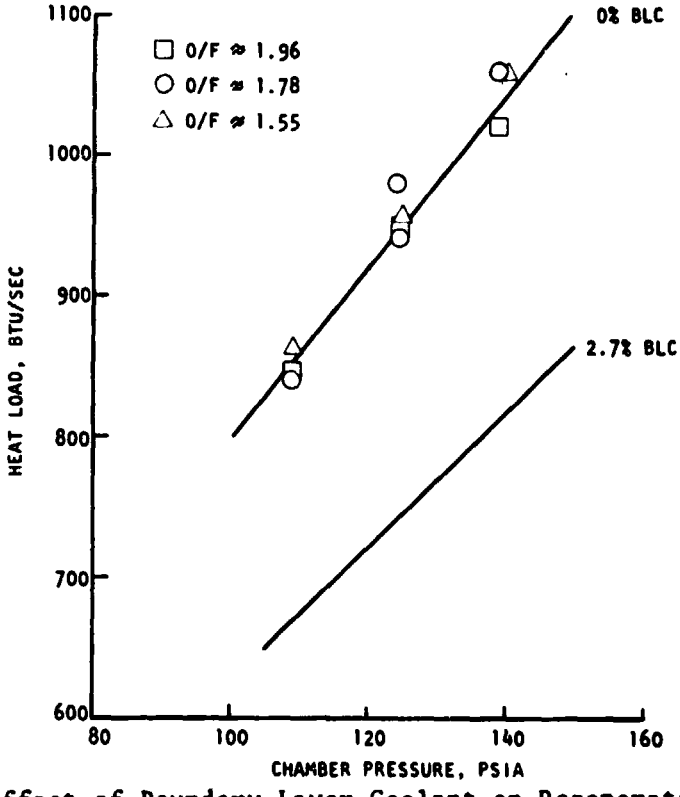


Figure 20. Effect of Boundary Layer Coolant on Regenerative Chamber Heat Load

Summarizing these tests, it appears that the ITC is capable of satisfactory operation for any duty cycle currently envisioned for the OME. Starts with simultaneous valve signal, restarts after coast times as low as 1 second and after tests as short as 0.1 seconds were accomplished without incident. The first two items result in minimum oxidizer lead times. The last item results in negligible heat input during firing and large propellant heat loss due to expansion and evaporation after shutdown. Restart after the short test, however, gave no indication of effects of possible propellant freezing. A fuel depletion test with helium ingestion was accomplished with no adverse effects on the chamber. Restart at maximum chamber soakout temperatures ( $\approx$ 500 F) were obtained without fuel decomposition or detonation.

Safety Factor and Fatigue Life

The ITC test results were utilized to improve the estimation of the chamber coolant safety factor and fatigue life profiles. This was accomplished by modifying the analytical models to fit the thermal data and then utilizing the models to predict heat lfux and wall temperature profiles.

The resulting safety factor profile based on 2-D conduction effects is presented in Fig. 21 for current off-design conditions with and without BLC. A minimum safety factor of 1.2 occurs near the injector end without film cooling. The ITC was not originally designed to operate without BLC. By simply increasing the velocity in the cylindrical section ($\Delta$P increase $\approx$ 2 psi) the safety factor could be increased to about 1.5.

Predicted fatigue life is 4800 and 4400 cycles for operation with and without BLC, respectively. This is in excess of the required life (4000 cycles with life safety factor = 4). The life could be increased further by annealing the high-strength electrodeposited nickel closeout to more evenly distribute the strain between hot-wall and closeout.

OME CHAMBER DESIGN OPTIMIZATION

The performance and thermal data obtained in this program allow for optimization of the thrust chamber design. The results of a parametric evaluation are shown in Fig. 22 . Performance could be maximized to about 313 seconds with a chamber length of 16.2 inches without supplemental film cooling. All coolant safety factor and minimum fatigue life requirements would be maintained.

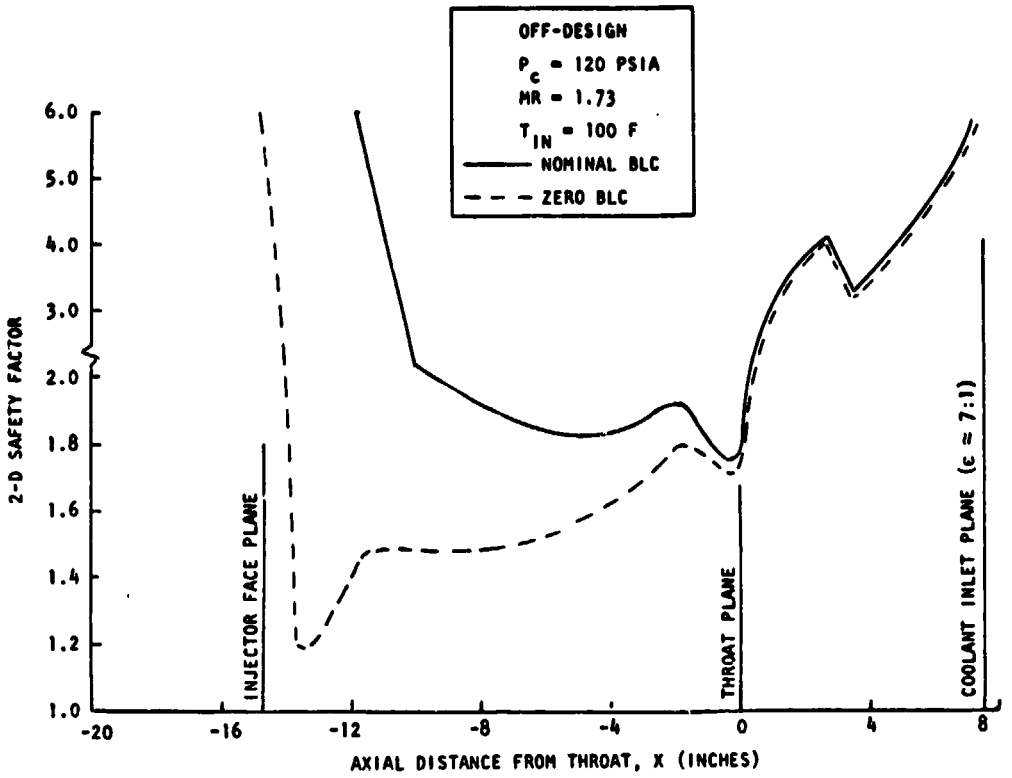


Figure 21. Regenerative Coolant Safety Factor Profile

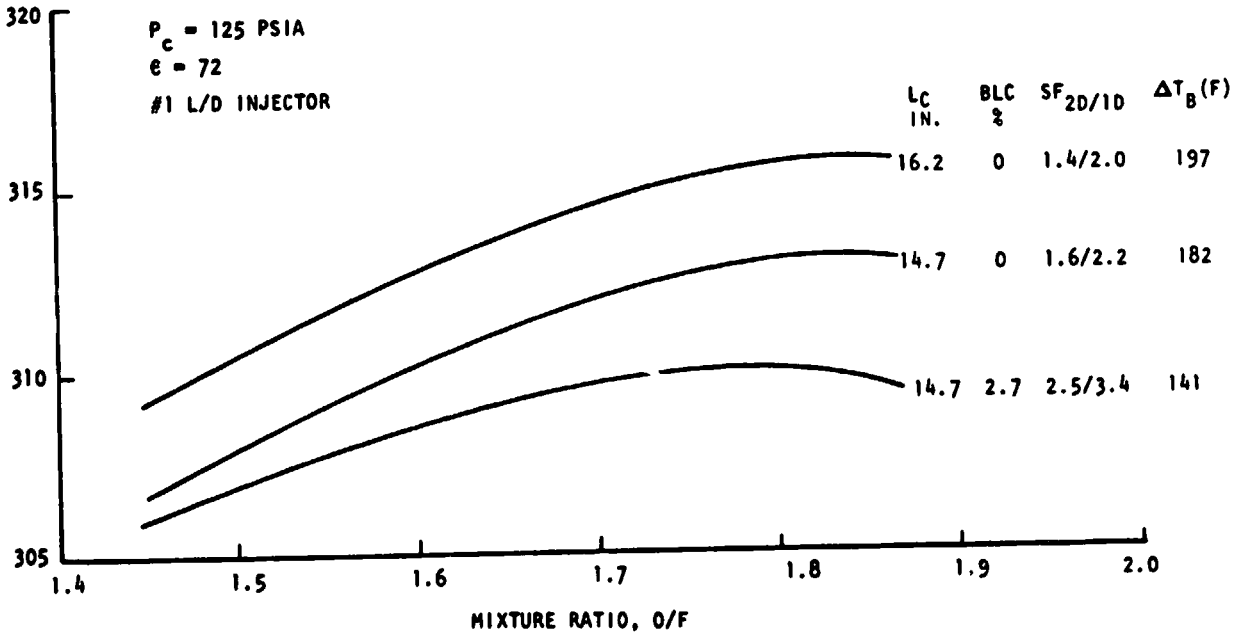


Figure 22. OME Performance with No. 1 L/D Injector

## CHAMBER DIAMETER COMPARISON

A comparison was made of 8- and 10-inch diameter chambers corresponding to nominal contraction ratios of 2 and 3, respectively. The effect of constant channel width versus constant land width fabrication technique was evaluated for the smaller diameter design. The three chamber configurations were designed and analyzed to determine pressure drops and channel height profiles. Weights were calculated for the chambers, injectors, and radiation nozzles. The chamber with the higher contraction area ratio is 2½ inches shorter than the other chambers so that a longer, higher performing nozzle can be used. Space Shuttle trade factors were used to convert differences in weight and pressure drop between the chambers to effective specific impulse differences. Combining these with the nozzle performance difference resulted in comparisons in performance between the three chambers for injectors with performance assumed to be equal. Alternatively, the injector performance requirements for equal effective specific impulse were determined.

### Results

The land width and height profiles required to maintain the required safety factor at off design conditions in the chamber having constant channel widths are shown in Fig. 23 . The channel width and height profiles for the chambers having constant land widths are shown in Fig. 24 . The jacket pressure drops and life expectancies are summarized below.

| Construction | $\varepsilon_c$ | Jacket $\Delta P$, (psi) | Life, (cycles) |
|---|---|---|---|
| Constant Channel | 2 | 7.7 | 5100 |
| Constant Land | 2 | 4.1 | 5100 |
| Constant Land | 3 | 3.9 | 4500 |

The pressure drop for the chamber with low contraction ratio and constant width channels is less than that measured on Rocketdyne's Demonstrator and Integrated thrust chambers because the latter were designed to accommodate a theoretical heat flux which was considerably higher than the experimental profile near the injector.

Jacket weights were calculated from the channel dimension profiles. Injector, coolant outlet manifold, and radiation nozzle weights for the high contraction chamber were scaled from the low contraction chamber weights. The resulting values (pounds) are tabulated below:

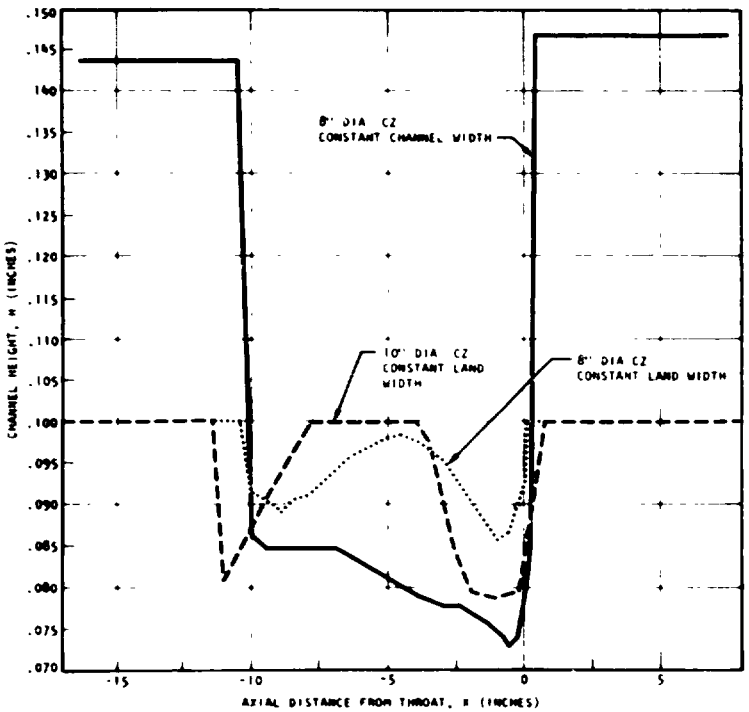


Figure 23. Channel Height Profiles for 8- and 10-Inch Diameter Chambers

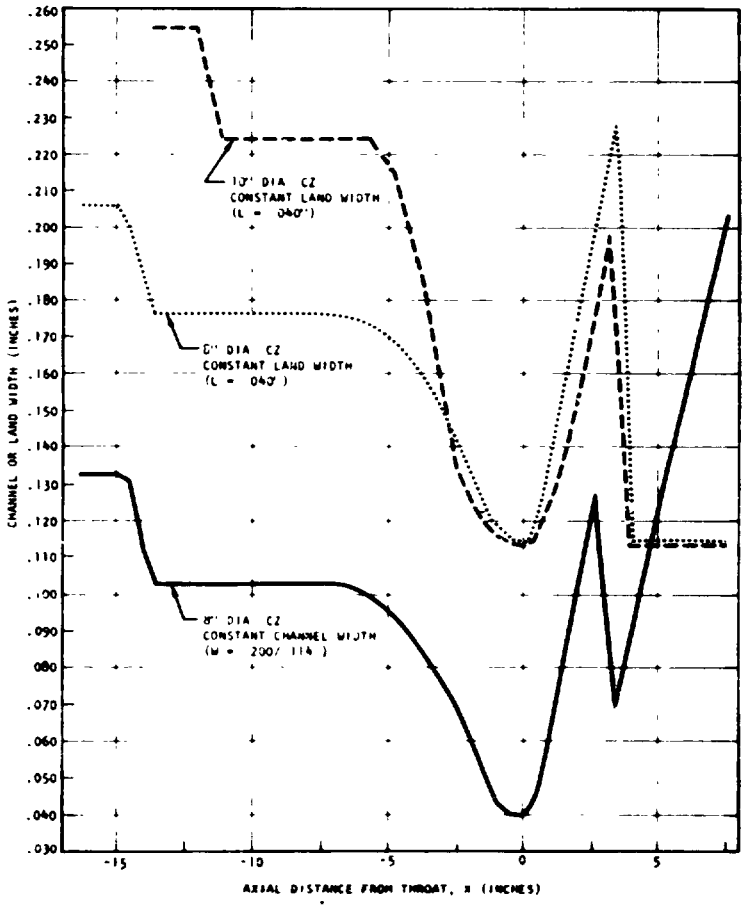


Figure 24. Channel or Land Width Profiles for 8- and 10-Inch Diameter Chambers

| Construction | $\epsilon_c$ | Jacket | Injector | Manifold | Nozzle | Total |
|---|---|---|---|---|---|---|
| Constant Channel | 2 | 24.0 | 23.6 | 11.4 | 41.2 | 100.2 |
| Constant Land | 2 | 17.5 | 23.6 | 11.4 | 41.2 | 93.7 |
| Constant Land | 3 | 17.0 | 35.4 | 12.1 | 42.5 | 106.8 |

The results presented in NASA Memorandum EP22/M11-74 were used to estimate the performance advantage of the longer nozzle used with the high contraction ratio chamber. The increment was 0.9 seconds specific impulse.

## Comparisons

Differences in weights and interface pressures were converted to effective specific impulse using the following OMS sensitivity data furnished by the NASA Program Manager

-4 lb system inert wt/psi interface pressure (oxidizer and fuel)

3 lb system inert wt/sec engine specific impulse

75 lb system wet wt/sec engine specific impulse

The results are summarized in Table 10 with comparisons made both on the basis of OMS wet weight and OMS inert weight. The chambers having constant width lands are superior to the chamber having constant width channels on either basis. The low contraction ratio chamber is significantly superior (3.2 seconds) on the basis of inert weight. Comparison based on OMS wet weight put more emphasis on performance so the longer nozzle of the high contraction chamber gives it a slight advantage (0.7 seconds).

TABLE 10. SUMMARY OF THRUST CHAMBER ASSEMBLY CHARACTERISTICS

| Configuration | $\epsilon_c$ | Wt. Difference Lb | Equivalent $I_s$, Sec | | Inlet Press., PSI | Equivalent $I_s$, Sec | | Nozzle $I_s$ Sec | Net Equiv. $I_s$, Sec | | Allowable Loss In $\eta_{c^*,s}$ | |
|---|---|---|---|---|---|---|---|---|---|---|---|---|
| Constant Channel Width | 2 | Nominal | Nominal | | Nominal | Nominal | | Nominal | Nominal | | Nominal | |
| | | | Inert | Wet | | Inert | Wet | | Inert | Wet | Inert | Wet |
| Constant Land Width | 2 | -6.5 | 2.2 | 0.1 | -3.6 | 4.8 | 0.2 | 0 | 7.0 | 0.3 | 2.2 | 0.1 |
| Constant Land Width | 3 | 6.6 | -2.2 | -0.1 | -3.8 | 5.1 | 0.2 | 0.9 | 3.8 | 1.0 | 1.2 | 0.3 |

## RECOMMENDATIONS

The stability and safety of injectors utilizing like-doublet elements in regeneratively cooled chambers was demonstrated in this program. Efforts should be made to improve the performance of this injector type while maintaining the present stability and safety characteristics. Cold flow tests of existing full-scale injectors should be made to establish mixing characteristics. Design and analysis efforts based on the cold flow results should be followed by injector subscale and full-scale tests.

Although the injector was stabilized by the proper acoustic cavity configuration, a 2600 hz oscillation has occurred with some cavity configuration on this and other programs. The persistance of this oscillation in some cases may be the result of a feed sytem interaction. This possibility should be further investigated in order to better understand and control the stability of the OME.

The LOX/MMH propellant combination was determined analytically to be a strong alternate candidate for the OME but was rejected primarily because of lack of experience. This propellant combination could be tested for future generation Orbit Maneuvering Engines using hardware fabricated during this contract - specifically L/D #1 which has provisions for an ignition system and the integrated thrust chamber.

## CONCLUSIONS

The analyses and tests conducted during this program lead to the general conclusion that a regeneratively cooled NTO/MMH engine can provide a lighweight, stable, propulsion system with high performance. Specific conclusions are best described in the order of the particular study areas.

The propellant and cooling method analyses lead to the conclusion that the regeneratively cooled NTO/MMH engine was the optimum of the various candidates studied based on considerations of performance, weight, development risk, cost, safety, maintainability, reliability, and air pollution. NTO/50-50, LOX/MMH, and LOX/50-50 were the alternate preferences in that order.

It was concluded from the subscale injector tests that the like-doublet injector would produce higher and more stable performance at OME operating conditions than injectors using either unlike-doublet or triplet elements. The highest performance could be obtained with a 45 degree cant angle and an impingment distance of approximately 0.4 inches. Mixture ratio, chamber pressure, and oxidizer temperature do not significantly affect C* efficiency which is limited by mixing more than by vaporization.

The thrust chamber cooling tests using electrically heated tubes and channels lead to the conclusion that regenerative cooling at OME design and off-design conditions can be accomplished with reasonable design parameters and factors of safety. Data obtained with simple round-tube data can be used to define steady-state safety factors for chambers using channel wall construction. The OME chamber can be started safely when hot due to a previous firing or heating by plume impingment from other engines. The chamber can tolerate large continuous helium bubbles in the fuel, but the safety factor is degraded by the presence of froth-like helium bubbles. The design of the cooling jacket would probably have to be modified to permit operation with a completely plugged channel.

The full-scale injector test programs demonstrated that a like-doublet injector provides safe, stable operation with moderately high performance. The injector can be stabilized with an acoustic cavity having a gradual contoured entrance. The conclusion from an analytical comparison of chambers using 8- and 10-inch diameter injectors was that, if the injectors provided equal C* performance, the resulting weight, pressure, and nozzle comparison resulted in higher system performance for the 8-inch chamber based on minimizing OMS inert weight. A slightly lower OMS tanked weight would result from the use of a 10-inch injector. The same study lead to the the conclusion that a chamber having lands of constant width was superior to a chamber having coolant channels of constant width.

It was concluded from the stability model tests and analysis that instabilities encountered in the frequency vicinity of 2600 Hz are probably due to the interaction of feed system dynamics and chamber acoustics. Chamber oscillating modes can be accurately predicted by model test data. The effective depth of the acoustic cavity is independent of the location of the downstream portion of the cavity.

The demonstrator chamber tests verified the analytical conclusions regarding safe engine operation at nominal and anticipated off-design conditions. In fact, it was concluded that the analyses were somewhat conservative regarding regenerative cooling safety factor and radiation nozzle temperatures. The fabrication of this chamber also demonstrated the feasibility of CRES channel-wall chambers using an electroformed nickel closeout. The feasibility of repairing certain types of chamber damage by electroforming was also demonstrated. It was concluded that the chamber could operate safely with NTO/50-50 propellants over the range tested at slightly higher performance than NTO/MMH provided.

Fabrication of a flightweight OME thrust chamber was demonstrated (excepting the inlet manifold) by the integrated chamber. Safe operation was demonstrated at nominal and anticipated off-design conditions with this chamber. The thrust chamber and injector can survive a fuel depletion condition and is stable in the blowdown mode to approximately 70 psia chamber pressure. Propellant saturation does not significantly affect either the performance or heat transfer characteristics of the engine. The L/D #1 injector in a 14.7-inch long chamber and a nozzle having an area ratio of 72 with 2.7 percent Boundary Layer Coolant provides 310 seconds specific impulse. Eliminating the BLC would increase performance by 1-1/2 seconds and still permit safe operation over the expected range of operating conditions. Simultaneously lengthening the chamber to 16 inches and eliminating the BLC would result in a specific impulse of 313 seconds and a thermal safety factor of 1.4 at nominal conditions.

Tests conducted with the integrated chamber and OMS simulated ducting lead to the conclusion that oxidizer depletion occurs within 10 seconds after engine shutdown for all anticipated operating conditions. Fuel depletion times range from one second after a long-duration test to 10 minutes after a 1-second test with cold fuel. Posttest accelerations in the order of 300 g's can result from low level combustion. These accelerations are not detrimental to the engine and can be avoided by a brief purge of the oxidizer system after shutdown. The engine does not impose any limitations on OMS restart times.